ADVANCED MATERIALS
www.advmat.de

Engineering Kirigami Frameworks Toward Real-World Applications

Lishuai Jin and Shu Yang**

The surge in advanced manufacturing techniques has led to a paradigm shift in the realm of material design from developing completely new chemistry to tailoring geometry within existing materials. Kirigami, evolved from a traditional cultural and artistic craft of cutting and folding, has emerged as a powerful framework that endows simple 2D sheets with unique mechanical, thermal, optical, and acoustic properties, as well as shape-shifting capabilities. Given its flexibility, versatility, and ease of fabrication, there are significant efforts in developing kirigami algorithms to create various architectured materials for a wide range of applications. This review summarizes the fundamental mechanisms that govern the transformation of kirigami structures and elucidates how these mechanisms contribute to their distinctive properties, including high stretchability and adaptability, tunable surface topography, programmable shape morphing, and characteristics of bistability and multistability. It then highlights several promising applications enabled by the unique kirigami designs and concludes with an outlook on the future challenges and perspectives of kirigami-inspired metamaterials toward real-world applications.

1. Introduction

Over the past two decades, we have witnessed the blossom of the design and fabrication of artificial metamaterials.[1–4] Unlike conventional materials, metamaterials derive their exceptional physical properties from elaborately engineered structures, leading to a new paradigm in material design across all length scales. Kirigami, the creative Asian art of paper cutting whose origins can be traced back thousands of years to when paper was first invented, has evolved as a powerful platform for scientists and engineers to create metamaterials with properties that have never been attained in the realm of materials science.[5–14]

The basic tenet of kirigami design is to embed functionalities into a flat thin sheet through rationally perforated cuts. Introducing an array of architected cuts into a thin sheet of material fundamentally alters its topology, giving rise to a significant change in the deformation mechanism compared to the original sheet. The deformation mechanisms of the kirigami structures can vary significantly based on several factors, including the geometry of the cutting motifs, the dimensions of the materials involved, and the applied boundary conditions. The ability to tailor mechanical properties based on these design parameters makes kirigami a highly versatile and promising tool to engineer materials with desired characteristics and applications. Considerable efforts have been made to investigate and optimize kirigami designs, with the aim to unleash their full potential across diverse fields, including soft robotics,[15–20] flexible electronics,[21–28] medical devices,[29,30] and energy storage.[31–34]

Owing to its profound relevance across a multitude of applications, there are several recent reviews that have surveyed this ever-evolving topic, providing a foundation for understanding kirigami designs. For example, Tao et al. have delved into comprehensive discussions about the mechanical characteristics that underpin kirigami-inspired designs.[14] Brooks et al. have explored the transformative potentials of kirigami-inspired healthcare applications.[12] Others have combined kirigami and origami designs to shed light on the multifaceted nature of kirigami, such as shape transformation,[6] 3D assembly,[7] and techniques in micro/nanofabrication.[5] Despite these insightful examinations, a gap persists in the practical application of kirigami principles to meet the demands of real-world challenges. Beyond achieving the desired functionalities, such as enhanced stretchability, target shape transformation, and tailored surface topography, it is imperative to consider a range of realistic factors, including the robustness within uncontrolled or even harsh environments,[35,36] the scalability and reproducibility in manufacturing processes,[37,38] and the pursuit of universal design methodologies for real-world applications.[39,40] In principle, the kirigami designs are scalable and material-independent. In practice, the intrinsic properties of the constituent materials cannot be ignored to ensure optimal outcomes in terms of high durability, robustness, sustainability, and cost-effectiveness. These considerations are crucial for the transition of kirigami frameworks from conceptual studies to practical, deployable solutions. Furthermore, given the rapid evolution of this field, a timely survey not only benefits the community but also catalyzes further innovations.

L. Jin, S. Yang
Department of Materials Science and Engineering
University of Pennsylvania
3231 Walnut Street, Philadelphia, PA 19104, USA
E-mail: jlstju@gmail.com; shuyang@seas.upenn.edu

The ORCID identification number(s) for the author(s) of this article can be found under https://doi.org/10.1002/adma.202308560

DOI: 10.1002/adma.202308560

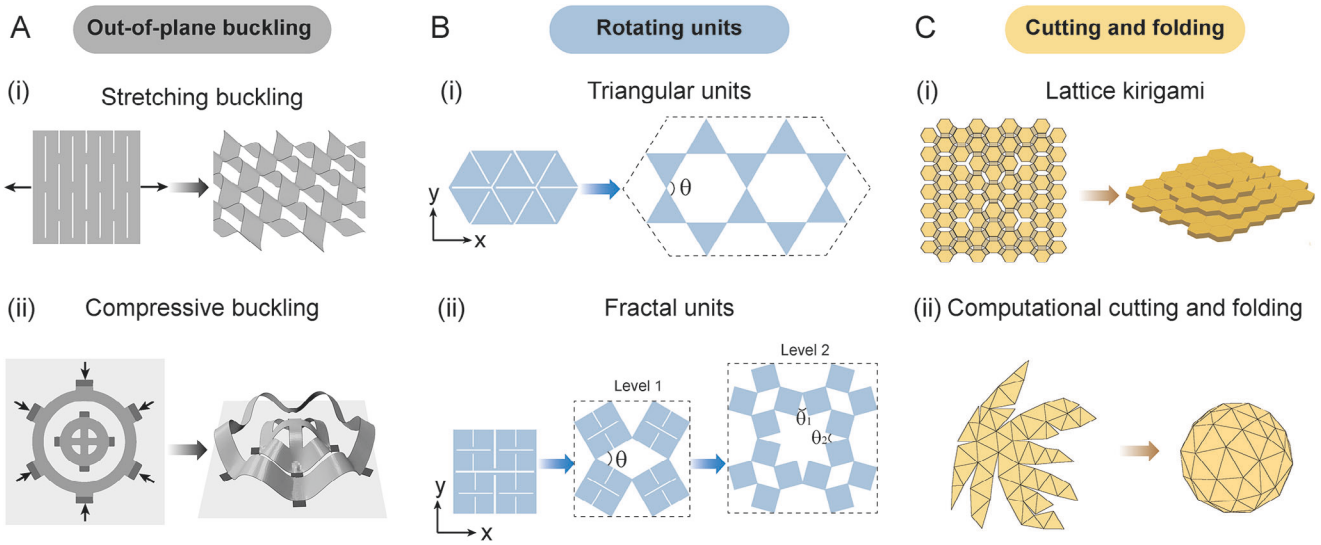

Figure 1. Deformation mechanisms of the building blocks in kirigami design. A) Out-of-plane buckling induced by (i) stretching and (ii) compression. B) Rotating-unit mechanisms can be harnessed to realize auxeticity and high stretchability. (i) Regular triangular units and (ii) fractal cut units. C) Incorporating cutting and folding enlarges the design space of kirigami. (i) The lattice kirigami and (ii) computational cutting and folding.

In this review, we focus on how to effectively apply kirigami design principles to address real-world challenges. We intend to establish a link between the kirigami structures and their distinctive properties, inspire the discovery of innovative kirigami-inspired metamaterials, as well as stress the practical deployments, motivating the research community to tackle the challenges presented by real-world problems.

The deformation of kirigami structures can be intricate; however, they predominantly rest on three fundamental mechanisms: buckling-induced deformation, rotating-unit mechanism, and the synergy of cutting and folding, as depicted in **Figure 1**. Collectively, these mechanisms confer kirigami with distinctive properties. In this review, we first present the basic deformation mechanisms inherent to various kirigami designs and explain the fundamental physics underlying the ever-improving properties of kirigami. Then, we outline the unique properties of kirigami that stem from rationally designed cuts, illustrating how each property can be utilized to foster advancements across diverse fields. Finally, we provide our insights on the challenges and perspectives to advance kirigami-inspired metamaterials to address real-world challenges.

2. Mechanisms and Design Principles of Kirigami

The pluripotent kirigami metamaterials are realized by perforating rational patterns into flat sheets, where their deformation mechanisms are governed by the cut patterns, the ratio of the critical size of the cuts (i.e., the hinge size or the distance between parallel cuts) to the sheet thickness, and the applied boundary conditions. Hence, the design of kirigami is intrinsically scalable and generically material-independent. The essential principle of kirigami lies in imparting nearly inextensible flat sheets with the ability to stretch, conform, and adapt. To this end, three main mechanisms are usually employed (Figure 1).

2.1. Buckling-Induced Deformation

By perforating flat sheets with rationally designed cuts, the resulting material possesses a significantly lower modulus than the pristine, uncut sheets. This mechanical compliance arises from the geometric nonlinearity induced by the cuts. In the case of a kirigami structure with parallel line cuts (Figure 1A(i)), a competition exists between in-plane deformation energy and out-of-plane bending energy when the structure is stretched. With a small amount of applied stretch, the in-plane deformation energy is smaller than the out-of-plane bending energy, leading to the structure deforming primarily within the plane. However, as the degree of stretching increases, out-of-plane deformation comes into play, which occurs when the in-plane and out-of-plane energies become equal. Notably, the out-of-plane deformation exhibits much lower stiffness than the in-plane deformation.[41–43] This is attributed to the fact that the bending modulus of thin sheets is considerably lower than their in-plane stretching modulus. However, as the applied strain approaches the stretching limit of the kirigami, the stiffness will rise again.

Much like stretching-induced buckling, compressing the cut sheets to a certain strain also results in out-of-plane deformation. This mechanism has been extensively employed in assembling elaborate 3D architectures at micro- and nano-scales.[44–48] The morphology of the resulting 3D structure is dictated by the geometry of the cut pattern and the applied boundary conditions. In order to accurately regulate the boundary conditions, compression is typically applied from another layer of pre-stretched elastomer. As shown in Figure 1A(ii), the dark gray rectangles indicate the bonding sites between the kirigami sheets and the pre-stretched elastomer. Releasing the stress in the elastomer induces compressive stress to these sites and buckles the kirigami sheets accordingly.

2.2. Rotating-Unit Mechanisms

The rotation mechanism offers another avenue to program deformation in 2D sheets, wherein the sheets are segmented into a collection of units (e.g., squares or triangles) linked at their tips.[49–51] The units separated by cuts are effectively rigid, while the connecting ligaments function like free-rotational hinges. The deformation of this type of structure is therefore determined by the kinematic relation between the units. For the kirigami design shown in Figure 1B(i), the strain of the structure can be calculated by the rotation angle θ of the triangular units and described by

$$\varepsilon_x = \varepsilon_y = \frac{2}{\sqrt{3}}\left(sin\left(\frac{\theta}{2}\right) + sin\left(\frac{\theta}{2} + \frac{\pi}{3}\right)\right) - 1 \quad (1)$$

Leveraging the rotating mechanism offers a compelling route to design auxetic structures. A broad spectrum of Poisson's ratios can be realized by fine-tuning the shapes of these rotating units.[52] Drawing inspiration from ancient Islamic arts[53] and wallpaper groups,[54] researchers have explored periodic units with irregular shapes, which impart bistability and programmable shape-shifting capabilities, significantly expanding the kirigami design space.

In addition, by embedding hierarchical cutting motifs within the sheets, one can achieve enhanced programmable deformations, as shown in Figure 1B(ii). These fractal cut designs permit substantially large strains and shape changes, which are contingent on the shape of the rotating units and the hierarchy level.[55] For level-1 hierarchy, the strain of rotating squares is given by

$$\varepsilon_x = \varepsilon_y = sin\left(\frac{\theta}{2}\right) + cos\left(\frac{\theta}{2}\right) - 1 \quad (2)$$

where the rotation angle θ is defined in Figure 1B(ii). The level-1 structure has only one degree of freedom, and increasing the hierarchy of the cuts results in more degrees of freedom in the structure. For a level-2 structure, two independent angles θ_1 and θ_2 determine the rotation of all units, and the lateral strain can be expressed as[55]

$$\varepsilon_x = cos\left(\frac{\theta_1}{2}\right) + \frac{1}{2}sin\left(\frac{\theta_1}{2}\right) + \frac{1}{2}cos\left(\frac{\theta_2}{2}\right) - 1 \quad (3)$$

$$\varepsilon_y = cos\left(\frac{\theta_2}{2}\right) + \frac{1}{2}sin\left(\frac{\theta_2}{2}\right) + \frac{1}{2}cos\left(\frac{\theta_1}{2}\right) - 1 \quad (4)$$

2.3. Combination of Cutting and Folding

Beyond the out-of-plane buckling, folding represents another pivotal method for transforming 2D sheets into 3D structures. Kirigami design involving cutting and folding emerged as a promising approach to conforming complex 3D structures. This technique blurs the boundaries between kirigami and origami, unlocking unique designs that cannot be achieved through cutting or folding alone. Notable instances include the lattice kirigami depicted in Figure 1C(i) and the computational cutting and folding showcased in Figure 1C(ii).

Lattice kirigami derives from the design of phyllotaxis and combines the techniques of cutting, folding, and regluing.[56] As shown in Figure 1C(i), a 2D sheet can be robustly manipulated into a complex 3D stepped shape by strategically removing topological discs from honeycomb lattice sheets. Compared to conventional origami design, this approach avoids the complexity of fold pattern design and the subsequent convoluted folding sequences. Remarkably, by varying the folding directions, a single lattice kirigami permits a wide variety of prescribed surfaces.[57–59]

The computational cutting and folding approach evolves from the unfolding of polytopes.[60] Specifically, a 3D mesh surface can be segmented into 2D patches without overlapping. These patches then serve as templates for cutting materials, which are subsequently folded back to reconstruct the original 3D shape.[61,62] Owing to the capability of transforming 2D sheets to arbitrary 3D configurations, this approach has been widely exploited in designing papercraft models[63–65] and self-folding structures[66–70] and applied in fields such as drug delivery[71] and robotics.[72]

Each mechanism described above unlocks immense potential for creating pluripotent metamaterials. The synergy of these mechanisms further amplifies the possibilities inherent in kirigami design. An et al.[73] employed the hierarchical rotating mechanism in conjunction with the buckling mechanism to create combined heterogeneous surfaces, which are capable of realizing tunable mechanical response and encrypting desired 3D patterns into flat sheets. By combining the folding and buckling mechanisms, numerous studies utilized rationally designed folding paths to guide the buckling morphology of 3D microstructures, providing new strategies for manufacturing 3D electromagnetic components across a wide range of length scales and material types.[47,74]

3. Unique Properties of Kirigami and Their Profuse Applications

The strategically designed cuts and folds facilitate the creation of diverse kirigami-inspired metamaterials, which exhibit unique mechanical,[41,53,75–77] thermal,[78–81] acoustic,[82–84] and optical[85–87] properties surpassing those of the original flat sheets. Here, we organize the functions of the kirigami designs into four primary categories based on their distinctive properties: high stretchability and flexibility, tunable surface topography, programmable shape morphing, and bistability and multistability (**Figure 2**). Since kirigami design principles are generally scalable and independent of specific materials, these unique properties can find applications across a wide range of fields. As such, they offer innovative strategies for achieving functionalities that conventional techniques fail to attain. In the following, we will provide an overview of the key properties of kirigami and explore how they are utilized to tackle challenges in various fields. We aim to offer a glimpse into the versatility and broad potential of this inventive approach, and guide the design of engineered materials for practical applications.

3.1. High Stretchability and Adaptability

One of the most prominent characteristics of kirigami is that it endows inextensible sheets with high stretchability and

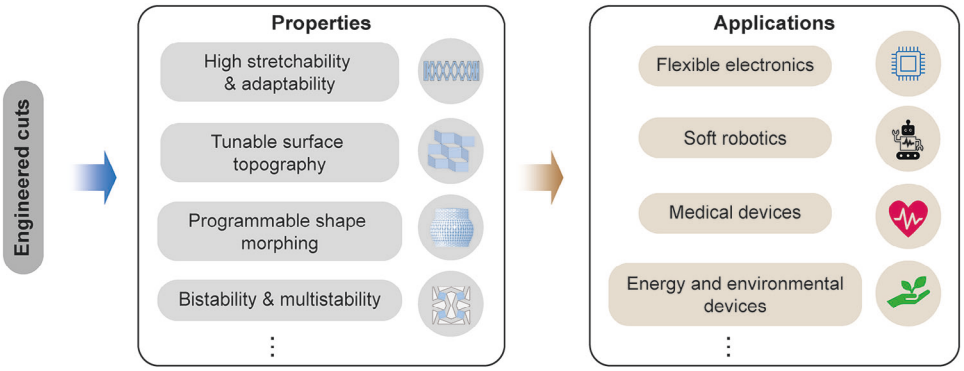

Figure 2. Rationally embedding cuts into flat sheets results in unique properties and diverse applications.

adaptability, which can be achieved by exploring the buckling mechanism, the rotating-unit mechanism, or a combination of both. Cho et al.[55] demonstrated how to leverage fractal cuts to engineer the super-stretchability and shape conformability of the cut materials. Conventional kirigami designs based on the rotating-unit mechanism have theoretical limits on the achievable strain. For instance, the maximum strain of the rotating squares, without stretching the ligaments, is 41.4%. In order to achieve larger programmable deformation, the authors incorporated hierarchical cutting motifs into the sheet, producing a fractal-architected design with significantly large stretchability. The maximum deformation is dictated by the cut pattern and the hierarchy level. For a square pattern with level-2 and level-3 hierarchies, the maximum strain is approximately 62% and 79%, respectively, which greatly exceeds the strain potential of the level-1 rotating squares without any hierarchy (**Figure 3**A). Moreover, the deformation characteristics can be precisely tailored by varying the hierarchical motif arrangement. In a homogeneously patterned structure, a level-4 hierarchical design facilitates a maximum strain of ≈ 108%. Intriguingly, a 90-degree rotation of the motifs at levels 2 and 4 results in a modified structure reaching a maximum strain of ≈ 130%, as depicted in Figure 3B(i). Further, non-uniform expansion properties are attainable within a level-3 hierarchy through heterogeneous integration of α- and β- motifs, with the degree of stretchability being programmable via selective incorporation of different hierarchical levels and motif types, as illustrated in Figure 3B(ii)).

The utilization of fractal cuts introduces a new strategy to empower rigid materials with extreme stretchability, facilitating the development of platforms for stretchable and flexible devices. Conventional approaches to producing flexible electronics rely on intrinsically flexible materials (e.g., elastomers) or engineered ultrathin inextensible materials (e.g., silicon) with wavy and serpentine structures. Kirigami has emerged as a complementary framework that can endow intrinsically inextensible materials with high stretchability and adaptability. Figure 3C demonstrates a prototype that leverages fractal kirigami to create flexible electrodes. By depositing a conductive film of multi-wall carbon nanotubes on a fractal-cut silicone rubber sheet, a light-emitting diode (LED) remains powered through the conductive film, even as the cut silicone rubber sheet is stretched over the contours of a baseball. This platform has since been extended to more sophisticated implementations such as auxetic displays[91] and shape-adaptive imagers.[92] Beyond the rotating unit mechanism, other kirigami-based mechanisms have collectively expanded the design space for flexible electronics. For instance, the out-of-plane buckling mechanism enables a translation of in-plane stretching to out-of-plane bending,[26,93] while the cutting and folding mechanism imparts exceptional adaptability.[94] Together, these mechanisms enrich the toolkit for engineering devices that exhibit extraordinary stretchability, seamless conformability, and enhanced sensitivity.

While substantial advancements in flexible electronics focus on conformability and sensing performance, their mechanical robustness should not be overlooked. On one hand, flexible electronics are prone to generate fracture and delimitations when subjected to large deformation. On the other hand, the working environments of electronics might be unpredictable and uncontrolled in practical applications, resulting in undesired damage to the components and compromising their functionalities. To circumvent these challenges, Liu et al.[35] developed a versatile materials platform based on a composite nanofiber framework and realized wearable kirigami electronics with high mechanical robustness and multifunctionalities (Figure 3D). This platform consists of a microporous framework based on aramid nanofiber composites, which exhibit high toughness to withstand stress concentration around kirigami cuts and prevent crack propagation due to the self-assembled hyperconnected fibrillar network. In addition, Figure 3E reports a strategy of combining rigid tiles and soft hinges to improve the robustness and survivability of the electronics in unpredictable environments.[36] This design replaces the hinges of rigid rotating units (e.g., Polyimide) with deformable, soft elastomers (e.g., silicone rubber K-704, Kafuter) to enhance structural conformability. The rigid tiles, on the other hand, can behave as armor to protect themselves and the underlying soft body from potential external physical damages without sacrificing the sensing capability. As a result, the device exhibits performance surpassing conventional electronic skin under various extreme conditions such as puncture, scratch, and thermal shock.

Furthermore, the kirigami principle can be applied to the design of flexible strain sensors with concurrent hypersensitivity and omnidirectionality. Subtle and abnormal vibrations generated from small cracks, corrosion, and loose screws may occur anywhere in any direction of engineering structures, such as buildings and bridges. The early detection of these issues can

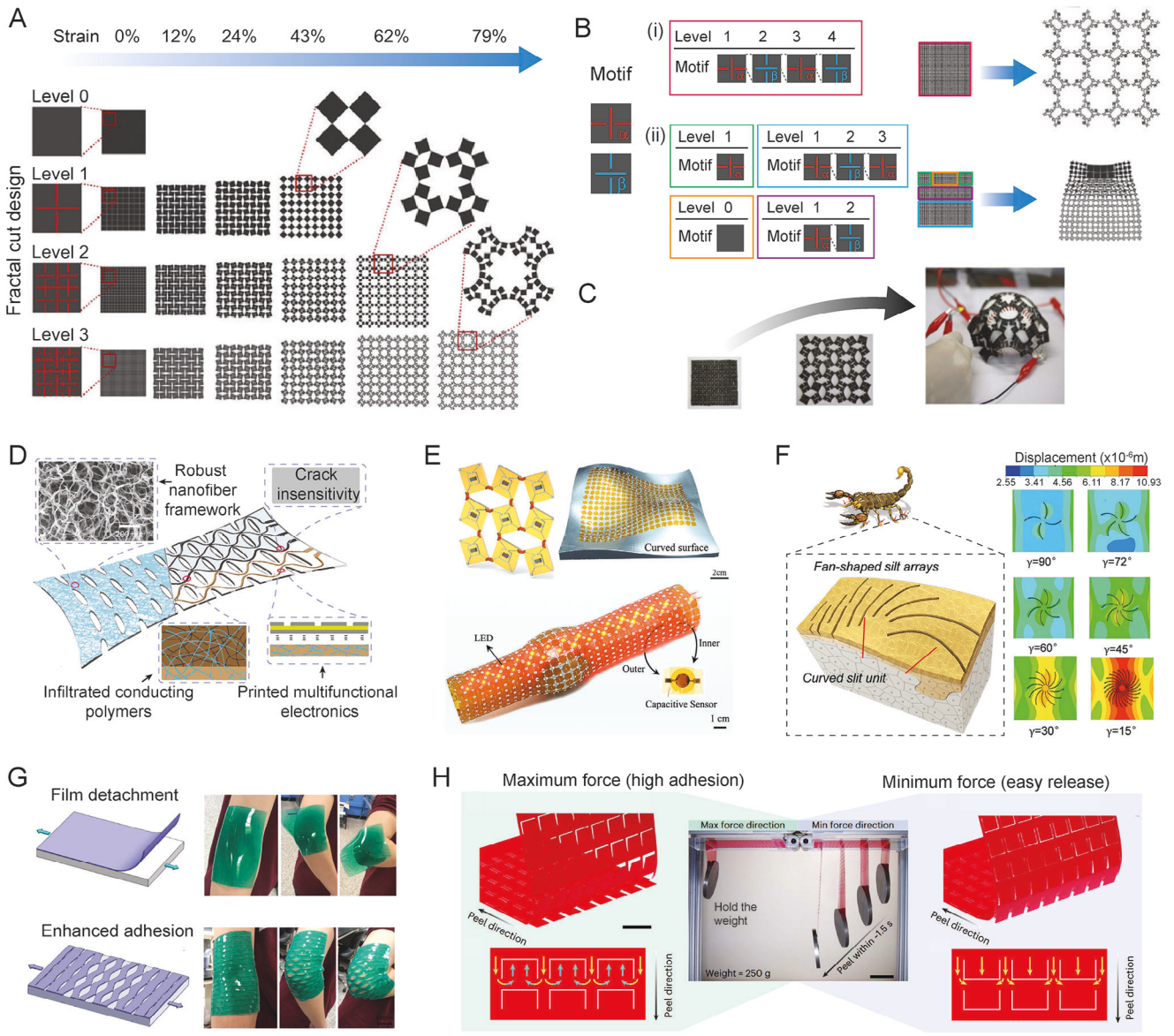

Figure 3. Highly stretchable kirigami and their broad applications. A) Auxeticity and high stretchability arise from fractal units. The finite element simulations of silicon rubber with finite size hinges reveal that the maximum strain of level-1, level-2, and level-3 designs are 43%, 62%, and 79%, respectively. B) Combination of different architectural motifs (α-motif and β-motif are 90° rotationally symmetric) gives rise to diverse stretchability. (i) A level-4 design with alternative α- and β-motif produces a maximum strain of 130%; (ii) Inhomogeneous deformation results from the mixing of motifs and the level of hierarchy. C) Prototype demonstration of a stretchable electrode platform based on fractal kirigami. The LED light remains lit after being conformed to a baseball. A–C) Adapted with permission.[55] Copyright 2014, National Academy of Sciences. D) Aramid nanofiber frameworks enabled kirigami electronics with high toughness, permeability, and manufacturability. Adapted with permission.[35] Copyright 2022, Wiley-VCH. E) Kirigami-based electronic armor capable of protecting itself and the underlying objects from potential damage. Adapted with permission.[36] Copyright 2022, Wiley-VCH. F) Bioinspired sensors leverage cuts and grooves to achieve omnidirectional and hypersensitive strain measurements. Adapted with permission.[88] Copyright 2022, Wiley-VCH. G) Kirigami enhances film adhesion due to its high stretchability and conformability. Unlike a continuous film, which tends to detach from the elbow during bending, the kirigami film maintains its adhesion. Adapted with permission.[89] Copyright 2018, Royal Society of Chemistry. H) High-strength, easy-release adhesives enabled by nonlinear cuts. The cuts result in 60x enhancement in adhesion from different directions. Adapted with permission.[90] Copyright 2023, Springer Nature.

prevent potential catastrophic disasters. However, it remains challenging to achieve so due to the anisotropy of sensing materials (e.g., nanotubes, nanowires, nanofibers) and their microscale patterning. The resulting sensitivity is always higher in the direction perpendicular to the cracks. Thus, measuring the orientation of the cracks often requires a pre-defined installation angle, which is not practical in real-world engineering applications. Figure 3F presents a bio-inspired approach that uses optimal cut patterns to determine the direction of the strain. Inspired by the sensing mechanism of vision-degraded scorpions, which can detect vibration stimulus presented 8 cm away at various angles by utilizing a slit sensillum with

fan-shaped grooves, Liu et al.[88] designed a flexible strain sensor composing curved microgrooves arranged around a central circle, exhibiting an unprecedented gauge factor of 18,000 in the strain range of 0.46%–0.65% for 7,000 cycles. By optimizing the geometry of microgrooves and laying the sensors in an array, it can sense various subtle vibrations of diverse input waveforms and discriminate the direction of the source, significantly enlarging the capability of existing strain sensors for on-site and fast localization of directional vibrations.

The high stretchability and unique topology of kirigami can also be exploited to enhance the adhesion between films and substrates. The conventional approach to ensure film-substrate adhesion involves making the films thinner, more compliant, and more adhesive, but such modifications may compromise the function or fabrication process of film–substrate structures. Figure 3G demonstrates an approach that enhances the film-substrate adhesion by introducing rational kirigami cuts in the films without changing their thickness, rigidity, or adhesive properties.[89] In contrast to the design of continuous poly(dimethylsiloxane) (PDMS) film (thickness, 1.5mm) bounded with a 10 μm adhesive layer (WACKER SiGel 613), which detaches from the Ecoflex substrate when stretched to λ (stretched length /original length) = 1.25, the kirigami film, possessing identical geometric and material parameters as the continuous film except for the cuts, remains adhered up to a stretch of $\lambda = 1.43$. Figure 3G visually contrasts the performance of both continuous and kirigami films when attached to an arm's elbow. In its straightened position, both films adhere effectively. During the act of bending, the continuous film delaminates easily, while the kirigami film exhibits strong adhesion even under severe bending (45°), with only slight delamination observed above the joint. This extraordinary adhesion performance results from the synergy of three factors: i) shear-lag effects, the edges of each kirigami segment undergo shear deformation prior to delamination upon stretching, which can delay the interfacial debonding; ii) partial debonding between films and substrates, which reduces energy release rate with interfacial crack propagation and prevents the full detachment of the film from the substrate; and iii) the compatible deformation of kirigami and substrates, which imparts reliable adhesion and conformability when the substrates undergo inhomogeneous deformation. Notably, the adhesion can be further programmed to achieve anisotropic adhesion[95] or simultaneously strong and releasable adhesion.[90] As demonstrated in Figure 3H, a kirigami adhesive exhibits reversible and directional adhesion characterized by securely holding a weight of 250 g in the maximum force peel direction while rapidly releasing it when applied in the opposite direction. This distinctive property is attributed to the nonlinear cuts, which effectively inhibit crack propagation by compelling cracks to propagate backward while facilitating crack growth in the opposite direction for easy release and reusability.

3.2. Tunable Surface Topography

Surface topography is crucial in determining the behavior and characteristics of engineered materials, impacting aspects such as tribology,[76,96] adhesion,[97] wettability,[98] and fluid dynamics.[99] This paves the way for a wide array of implications across diverse sectors, including soft robots,[100] biomedical implants,[101] and photonic and phononic crystals.[82,102] Conventional methods to achieve various surface topographies employ techniques like photolithography, additive manufacturing, micro- and nano-machining, and self-assembling. Kirigami, as a complement to other techniques, offers a scalable technique to craft intricate 3D surface topographies across various length scales, demonstrating its potential to address practical challenges.

To tackle the global water shortage crisis, harvesting fresh water from environmental sources such as fog emerges as a promising solution. Yet, traditional fog collectors are inefficient due to aerodynamic deviation, where the viscous drag of fog-laden wind is deflected around or intercepted by the collecting surface.[103–105] On the other hand, when micro- and nanostructures are introduced to improve the transport and drainage of fog droplets on surfaces, the collectors are not only expensive to fabricate but prone to physical damage and biofouling, making them unsuitable for applications in an outdoor setting.

Li et al.[37] introduced a transformative strategy for fog collection based on kirigami-induced surface topographies. This method is capable of achieving not only high water collection efficiency but also robustness in complex environments, and it is adaptable to meter-scale manufacturing and deployment. As demonstrated in **Figure 4**A, this collector utilizes aerodynamics-assisted fog interception stemming from the geometric curvature, along with directed droplet gathering induced by the asymmetric morphology, to attain exceptional water collection efficiency. The kirigami surface consists of 3D pyramid units separated by selectively patterned openings. The conjunction of geometric curvature with openings can regulate the wind flow, forming counter-rotating vortices around the substrate (Figure 4B). These vortices flutter back and forth around the fold and accumulate fog droplets inside the vortices, thereby guiding the trajectories of fog droplets laden in the air and efficiently directing them to the substrate. As a result, extensive droplets with diameters > 500 μm emerge on the cubic kirigami with a folding angle $\theta = 150°$, whereas droplets of smaller diameter < 300 μm dominate on the 2D perforated surface.

Additionally, intercepted droplets can be guided by asymmetric channels formed by folds, as depicted by the experimental snapshots in Figure 4C. When the droplets at the edges grow large enough, they fall in an avalanche-like manner, gathering substantial droplets from the central region of each facet. They are then guided along the valley channel and eventually drip from the bottom tip of the concave pyramid. These combined advantages result in a fog collection efficiency ≈ 16.1% at a low wind speed of 0.8 ms^{-1}, which is 2.7 and 1.8 times those from the state-of-the-art fog collectors, wire mesh, and Raschel mesh, respectively, under the same experimental conditions (Figure 4D).

Notably, the high water collection efficiency rendered by kirigami surfaces is primarily governed by the 3D surface topography, not surface texture or surface chemistry. Hence, it is robust against physical and chemical fouling and can be applied to a broad diversity of low-cost materials and sheets. The experimental investigation has revealed that the pyramidal kirigami, irrespective of the material or surface treatment, consistently maintains an average water collection rate of ≈ 17.5 L/(m^2.h) as long as the apparent water contact angle remains

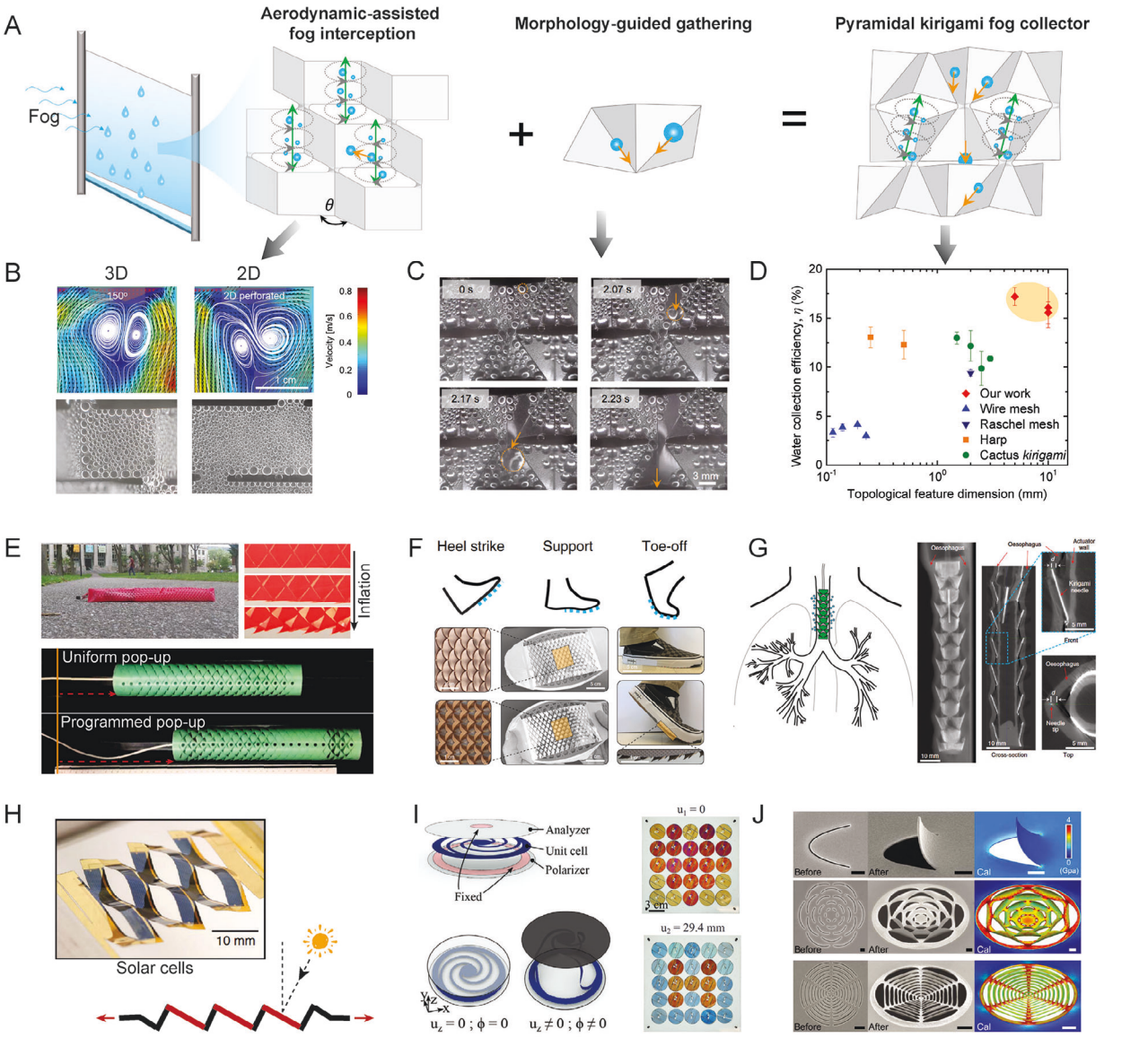

Figure 4. The unique 3D surface topographies of kirigami empower profuse applications. A–D) Aerodynamic-assisted fog collector with high efficiency. A) Schematic illustrations depict the mechanism of the fog collector. This collector leverages aerodynamics-assisted fog interception, which is induced by the geometric curvature and the directed droplet gathering, brought about by the asymmetric morphology, to attain remarkable water collection efficiency. B) Top: the velocity field of fog-laden air around the cubic kirigami surfaces with folding angles $\theta = 150°$ and $\theta = 0°$, respectively. A pair of counter-rotating vortexes emerge around the mountain fold, generating additional stagnation regions in front of the curved substrate, which enhances the deposition of droplets onto the substrate. Bottom: the diameter of droplets at the center of the cubic facet is much larger than those on the perforated surface without folding. C) Experimental snapshots validate the transport and dripping of droplets rectified by the valley folds. D) The comparison of the collection efficiency of various fog collectors. Compared to conventional fog collectors, the conjunction of effective fog interception and directed transport enables significantly higher water collection efficiency in larger-scale structures. A–D) Adapted under the terms of the Creative Commons CC-BY license.[37] Copyright 2021, The Authors. Published by Springer Nature. E) The out-of-plane deformation of kirigami creates unique surface topographies that can be harnessed to produce directional frictional properties, thereby enhancing the locomotion efficiency of crawling robots. Kirigami sheets: Adapted with permission.[16] Copyright 2018, The American Association for the Advancement of Science. Kirigami shells: Adapted with permission.[106] Copyright 2019, National Academy of Sciences. F) Steel kirigami surfaces for friction modulation in footwear. The kirigami sheets buckle out-of-plane during walking to enhance the frictional properties and prevent slips and falls. Adapted with permission.[76] Copyright 2020, Springer Nature. G) Kirigami-inspired stents for sustained local delivery of therapeutics, which can deposit drug depots in the gastrointestinal tract across millimeter to multi-centimeter length scales. Adapted with permission.[30] Copyright 2021, Springer Nature. H) Kirigami-based solar cells offer a solution for integrated solar tracking. Both the tilting direction and angle can be precisely adjusted to optimize optical tracking efficiency. This method rivals the performance of conventional trackers while remaining simple, cost-effective, and lightweight. Adapted with permission.[107] Copyright 2015, Springer Nature. I) Chiral mechanical metamaterials transform a linear displacement into twisting, enabling mechanical pixels that can modulate the transmission of light through deformation. Adapted with permission.[108] Copyright 2023, Wiley-VCH. J) Nano-kirigami structures implemented by in situ cutting and buckling of suspended gold films with programmed ion beam irradiation, resulting in giant optical chirality due to the nanoscale 3D twisting features. Scale bars, 1 μm. Adapted with permission.[85] Copyright 2018, The American Association for the Advancement of Science.

under 150°. Remarkably, the design can be scaled up to 1 m^2 or even larger when meter-scaled modules are assembled together (e.g., 2 x 2 m^2), offering more practical, low-cost, and deployable solutions for fog water collection despite diverse real-world constraints such as local wind speeds, cost concerns, footprint, and availability of local materials for deployment.

Soft machines and actuators, with their intrinsic flexibility and compliance, are particularly suited to navigate complex and unstructured environments. However, their locomotion often necessitates the use of multiple actuators that operate independently.[109] Figure 4E demonstrates a bio-inspired strategy to circumvent this challenge. It utilizes 3D textured surfaces produced by kirigami to simplify the locomotion control of soft robots while ensuring it to remain efficient.[16,106] The crawling robot consists of an extensible actuator enveloped by a kirigami skin. Upon pneumatic inflation, the actuator extends and drives the kirigami skin to deform out-of-plane, leading to a dramatic change in the friction properties of the crawling robot. This feature is akin to the scaled skin of snakes, which produces directional friction due to the asymmetric pop-up deformation, enabling efficient crawling with simple controls. When curvature is incorporated into the kirigami skin, the pop-up features can be further programmed. Adjusting both the curvature and ligament size within the kirigami units allows for a controlled, sequential pop-up deformation. As illustrated in the bottom panel of Figure 4E, the pop-up deformation of the programmed kirigami shell first emerges at the two ends upon inflation and then propagates from one end to the other. This programmed deformation enhances the anchorage of the crawler to the substrate at both ends and significantly reduces the backslide. As a result, the crawler with programmed skin proceeds about twice as fast as those with a homogeneous pop-up deformation.

The pop-up feature of kirigami has been further applied to footwear outsoles, leading to enhanced friction forces in the forefoot and transversally to the direction of movement.[76] Falls, with their associated complications, pose significant health risks to older adults. Drawing inspiration from natural structures like claws and scales, Figure 4F showcases slip-resistant kirigami grips that can be attached to the footwear soles to reduce the risk of falls. During walking, the bending of the shoe soles causes stretching in the attached patches prompting the spikes to buckle outward. The elaborately engineered geometry of the kirigami patches enables a dynamic friction modulation: they remain flat with the sole when the wearer is standing still but enhance friction during walking, presenting a promising solution to prevent slips and falls across various environments.

These pop-up features also find applications in biomedical therapeutics, notably in the form of kirigami-based stents. Implantable drug depots, capable of satisfying therapeutic needs in a localized manner, can effectively enhance the potency of the drug at the target site while reducing the risk of possible side effects elsewhere in the body. However, the anatomic distribution of localized drug delivery for tubular organs, such as the gastrointestinal tract, remains challenging with existing therapeutic modalities. These limitations range from complications such as stent migration and tissue perforation to insufficient drug diffusion through the tissue layers. To overcome these challenges, researchers introduced a kirigami-based drug-releasing system (Figure 4G), which can provide a rapid circumferential and longitudinal submucosal drug deposition.[30] The kirigami-based stent consists of a cylindrical kirigami shell for drug deposition and a pneumatic actuator to trigger the delivery. Upon inflating the actuator, the kirigami shell will be stretched and buckled outward, such that the kirigami units undergo a change in orientation from planar to perpendicular to the stent body surface. The radial expansion of the stent can achieve up to 60% of the original diameter, and the buckled kirigami units function as denticle-like needles, enabling submucosal injections of drug-loaded degradable microparticles. By rationally designing the geometry, the kirigami-based injectable stents can deposit drug depots circumferentially and longitudinally in the tubular organs across millimeter to multi-centimeter length scales, including the esophagus, blood vessels, and airways.

Another implementation of kirigami-based surface topography is optical manipulation across various scales. For instance, the out-of-plane buckling-induced tilting effect in the kirigami units can be strategically utilized in designing solar panels. To optimize electrical power production throughout the day, traditional flat panel solar cells frequently employ optical tracking systems, which are intricate and require expensive and bulky structural parts to bear the weight. Kirigami provides a simple, low-cost, and lightweight solution to circumvent this challenge and maximize solar power generation. Figure 4H demonstrates that by embedding an array of rationally designed cuts into thin-film solar cells, instability-induced structural tilting can be leveraged to track the sun.[107] Importantly, the tilting angle can be precisely adjusted by varying the stretching amplitude, and the tilting direction be readily tuned by lifting or lowering one end of the sheet prior to the straining process. This mechanism has been further adapted to dual-axis tracking systems and applied to large-scale solar concentration.[110] Beyond leveraging the buckling-induced tilting intrinsic to kirigami, Forte et al. demonstrated the use of chiral kirigami cells inspired by Archimedean spirals to convert linear displacements into twisting motions.[108] The interaction between the extension and twisting endows the chiral cells with an array of highly nonlinear behaviors. By integrating these units with polarizing films they realized mechanical pixels capable of modulating the transmission of light through deformation, which have been further arranged in 2D arrays to realize color displays (Figure 4I).

While mesoscopic kirigami techniques predominantly find applications in the mechanical or acoustic domains,[111,112] the diverse geometries offered by nano-kirigami pave the way for applications in nanophotonics.[85] As illustrated in Figure 4J, an one-step approach has been developed to achieve nano-kirigami. This method employs in situ cutting and buckling of a suspended gold film using programmed ion beam irradiation. This results in a complex 3D shape transformation, manifesting in features such as buckling, rotation, and twisting of the nanostructures. Notably, these nanoscale 3D twisting configurations facilitate pronounced optical chirality, which is in significant contrast to the achiral 2D precursor that lacks the engineered 3D topography.

3.3. Programmable Shape Morphing

Shape-morphing structures are materials or systems designed to change their shapes in a controllable manner in response to

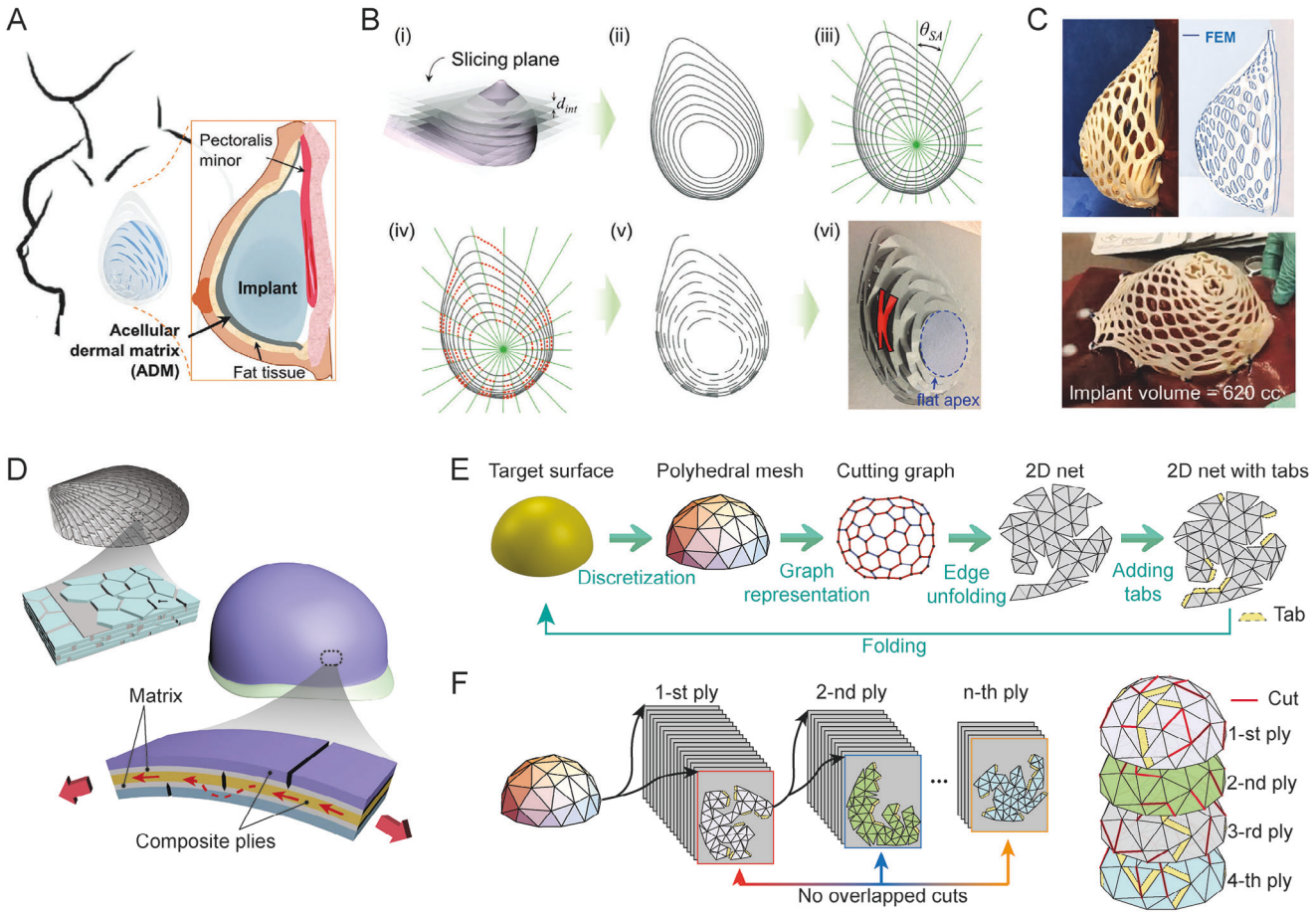

Figure 5. Shape-morphing structures empowered by programmable kirigami. A–C) Implant-based breast reconstruction utilizing fractal and contour cut kirigami. A) Schematic illustration of kirigami-engineered wrapping process for breast reconstruction. B) The topographical information of the breast can be embedded into the kirigami via an algorithmic design process. C) Finite element (FE) analysis and experimental demonstration of the Keller Funnel insertion process with the optimized kirigami sheets. A–C) Adapted with permission.[123] Copyright 2023, Wiley-VCH. D–F) Nacre-inspired shape-morphing strategy for high mechanical stiffness and strength. D) The mechanism of this approach is realizing the shape-shifting to prescribed shapes along with mimicking the staggered architecture of nacre shells for high mechanical properties. E) Schematic illustration of unfolding a target doubly-curved surface to valid 2D networks, which in turn can be wrapped to approximate the target shape. F) Illustration of the algorithm, which prevents cuts from overlapping at the same position in the shell. D–F) Adapted with permission.[38] Copyright 2022, The American Association for the Advancement of Science.

external loads or stimuli. These structures have gained significant interest in recent years due to their potential applications in various domains, ranging from medical devices[113] and soft robotics[114] to aerospace[115] and civil engineering.[116] Conventional shape-morphing materials primarily rely on deformable elastomers, attaining specific shapes in response to stimuli such as pneumatic inflation,[117,118] heat,[119] light,[120] or the application of electronic or magnetic fields.[121,122] In contrast, kirigami empowers almost any inextensible sheet material with the ability to transform into desired configurations through strategic cutting and folding.

Tissue-reinforced acellular dermal matrices (ADMs) are widely utilized in breast reconstruction for patients who have undergone mastectomy prophylactically due to breast cancers. However, a single ADM sheet cannot completely and conformably wrap the implant without wrinkles or voids. Not only it costs more materials to wrap the implant, but the appearance of the implant is not natural, and it is prone to mispositioning. Lee et al.[123] circumvent this challenge by combining contour cuts that prescribe the topographical height and fractal cuts in the center that ensure horizontal expandability (**Figure 5**A). The morphological information of the breast can be encoded into the kirigami design via a computational design process, as shown in Figure 5B. By optimizing the contour cuts using finite element simulations and considering the elasticity of ADM, the kirigami design is able to produce a natural teardrop shape under the self-weight of the implant, along with minimizing gap openings and reducing localized mechanical strain to prevent tearing of the ADM sheets during operation. This is accomplished by fine-tuning geometric variables, including slicing angles, the ratio of cut length to margin, and the spacing between contour lines. The effectiveness of this method is exemplified in a mockup operation employing a laser-cut kirigami ADM sheet (as shown in Figure 5C), where natural shapes are achieved using round implants with variable volumes (400 cc to 620 cc). The initial round shape mitigates the undesired appearance when the unsecured implant pivots

during movement. Beyond achieving a successful and aesthetically pleasing breast reconstruction, the kirigami technique also presents significant economic advantages, reducing an estimated 50% of material costs.

While engineered cuts grant kirigami sheets remarkable stretchability and conformability, these alterations inherently weaken the materials. It's undeniable that there's an essential need to produce desired 3D shapes from 2D materials without compromising their mechanical robustness and stiffness, particularly in aerospace and automotive engineering. Drawing inspiration from the architecture of nacre shells, Figure 5D–F details an optimal and universal cutting and stacking strategy that transforms composite layers into 3D doubly curved shapes with high stiffness and strength.[38] Nacre shells exhibit extraordinary mechanical strength and toughness in comparison to their artificial counterparts due to the ordered hierarchical architectures and the abundant interfacial interactions. By emulating nacre's architecture, the cutting patterns of kirigami can be optimized layer by layer to produce a multilayered laminate with staggered cut distribution. This design strategy exploits interlaminar shearing to mitigate the mechanical weakness induced by the cuts, as depicted in Figure 5D.

To realize the potential to morph into any prescribed shape, an algorithm is developed to unfold any given 3D surface into non-overlapping 2D nets (Figure 5E). Specifically, a target surface is first discretized into a polyhedral mesh, which can then be represented using a 2D cutting graph and further unfolded into 2D nets employing a minimum spanning tree approach. Varying the weight of each edge in the cutting graph gives rise to different 2D nets, which permits the optimization of the distribution of the cuts in the multilayered 3D structures. Crucially, when an edge has been cut in previous layers, it will not be cut again in subsequent ones for a finite number of layers. This procedure ensures that no cuts overlap at the same position, guaranteeing a homogeneous distribution of cuts across the multi-layered 3D structures (Figure 5F). The effectiveness of this approach is validated via several experimental tests, including assessing the performance of hemispherical shells and face guards fabricated from a high modulus bidirectional laminate, Tensylon HSBD30A (DuPont TM) plies. Tensylon is a fabric film made from ultrahigh molecular weight polyethylene (UHMWPE) with two orthogonal layers of solid-state extruded fibers coated with adhesives, which can be thermally cured to set the shape. However, due to its high in-plane shear stiffness, conventional solid-state extruded films such as Tensylon cannot easily be shaped into a hemisphere without wrinkling or tearing. In comparison to their randomly designed counterparts, the optimized samples, enhanced with additional tags, display considerably increased peak forces and stiffness under various boundary conditions, thereby highlighting the potential and effectiveness of the algorithm.

To facilitate the transformation of kirigami sheets from 2D to 3D, the introduction of a gradient is crucial. When such a gradient is implemented, the deformation of the kirigami sheets becomes non-uniform. If the deformation maintains 2D compatibility, the sheets merely deform within a two-dimensional plane, affecting only the boundaries of the sheets. Differently, when the deformation exceeds 2D compatibility, it triggers out-of-plane buckling and deforms to a 3D shape. However, how to develop a closed, compact regular kirigami tessellation to conform to a prescribed target shape in 2D or 3D was elusive until Choi et al.[124] presented their inverse design model based on the rotating-unit mechanism. This model employs a flexible constrained optimization framework, where the number, size, and orientation of cuts are optimized under the constraints of the lengths and angles of generalized kirigami tessellations. As a result, approximately any predefined 2D and 3D configurations can be reversely engineered from closed and compact kirigami tessellation, as shown in **Figure 6**A. A different strategy utilizes non-periodic cut patterns to buckle sheets into 3D shapes.[125] These shapes are induced by geometric frustration resulting from non-periodicity and can be rationalized by an in-plane kinematic analysis. Such methodologies contribute foundational elements to the construction of shape-morphing mechanical metamaterials.

Most kirigami-inspired shape-morphing structures have cuts or voids when deployed, preventing them from being airtight. This restriction hinders their use in inflatable shape-morphing designs, which are prominent in soft robotics,[128,129] assistive devices,[130] and camouflages.[117,131] Figure 6B introduces a solution that combines non-periodic kirigami cuts with flexible elastomers, paving the way for pneumatically activated kirigami structures with programmable shapes. Unlike conventional kirigami patterns marked by slender slits, this design involves wide cuts, mediating the deformation mismatch between kirigami and elastomers. Given that the modulus of the kirigami sheet is substantially larger than that of the elastomer ($\approx 10^5$ times), the structure's deformation is predominantly determined by kirigami geometry, specifically the unit cell's aspect ratio H/L and the normalized hinge size δ_1/L. Meanwhile, the elastomer imparts the structure with airtightness, enabling pneumatic actuation through the injection of compressed air. This allows the structure to morph into various predetermined shapes at a given pressure. Additionally, the tessellated nature of kirigami design permits individual manipulation of each unit cell's geometry, facilitating the accurate replication of target shapes across different scales.

Kirigami originates from the art of paper cutting but has evolved to incorporate folding, thereby exploring previously untapped territories in the materials design space. For instance, while many kirigami-based techniques lead to shape morphing to prescribed shapes, few of them can realize multiple shapes within a single design. Figure 6C demonstrates a lattice kirigami design, which realizes various prescribed surfaces within a single pattern by simply altering the folding directions. This design consists of an array of disclination defect pairs on the dual to the honeycomb lattice, leading to a manageable set of allowed motifs, including $2-4$ disclination pairs on a honeycomb lattice that has twofold and fourfold coordination, $\tilde{5}-\tilde{7}$ disclination pairs on a triangular dual lattice that has fivefold and sevenfold coordination,[56] and sixon, where a defect is formed by completely removing one hexagon from the honeycomb lattice.[57] For the sixon lattice shown in Figure 6C(i), by choosing the excised hexagon centers to lie on a triangular lattice, the fold patterns required by the placement of multiple sixons can be designed commensurate. Thereby, the triangular lattice of sixons can be readily designed to match a target surface approximately. As shown in Figure 6C(ii), the same triangular lattice of sixons can be used to approximate both a monkey saddle and the topographic features of Mountain Katahdin, among many other examples.

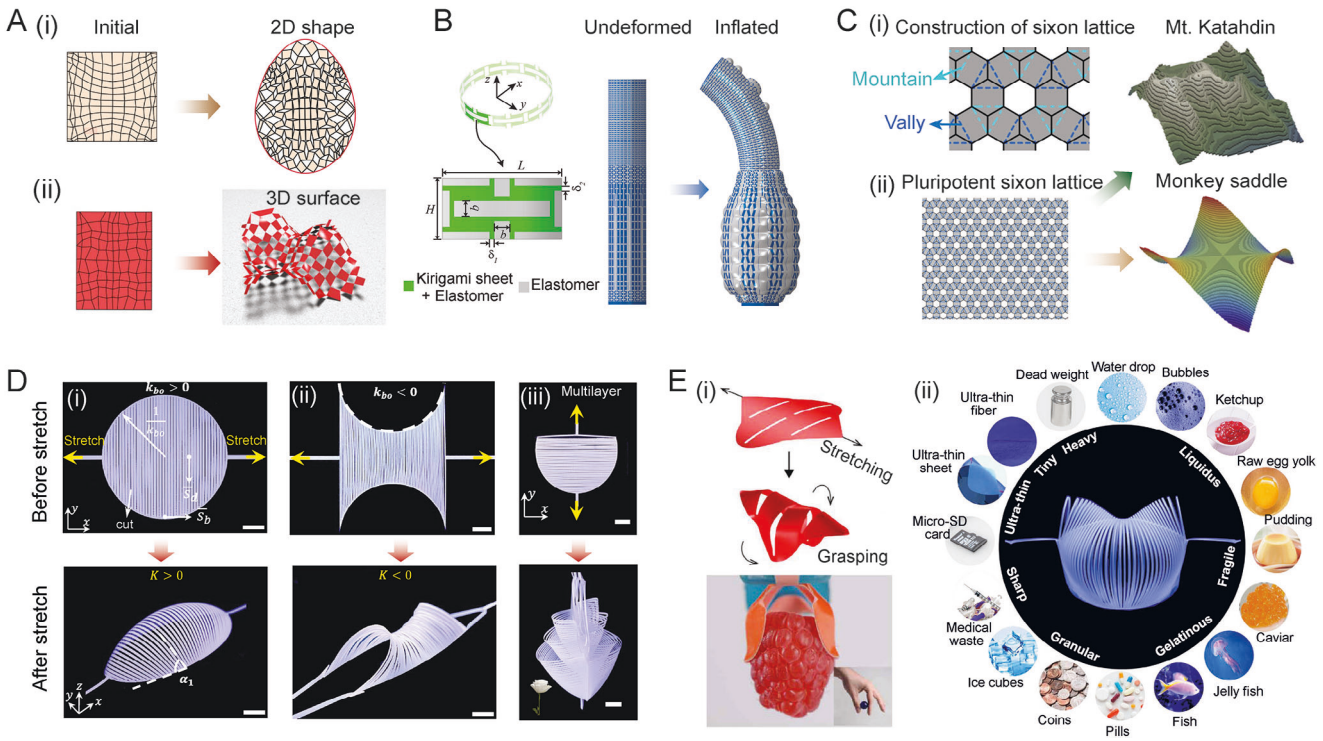

Figure 6. Tessellated kirigami enables dynamic shape-morphing structures. A) An inverse design approach to approximate arbitrary shapes in 2D and 3D from closed and compact rotating units. Adapted with permission.[124] Copyright 2019, The Authors. Springer Nature. B) Embedding rationally designed kirigami sheets into unstructured elastomers produces inflatable structures that permit desired shapes upon application of a certain pressure. Adapted with permission.[126] Copyright 2020, Wiley-VCH. C) Conjunction of cutting and folding enables pluripotent lattice kirigami designs, which permit a wide variety of target surfaces within a single lattice design. Adapted with permission.[57] Copyright 2015, National Academy of Science. D) Shape-morphing kirigami sheets guided by boundary curvatures. The sheets are composed of parallel discrete ribbons enclosed by continuous boundaries, which, upon stretching, buckle to target 3D shapes including (i) positive Gaussian curvature, (ii) negative Gaussian curvature, and (iii) multilayered flowers. Adapted under the terms of the Creative Commons CC-BY license.[19] Copyright 2022, The Authors. Published by Springer Nature. E) Shape-shifting kirigami sheets empower the design of soft grippers. (i) The concept of using kirigami to design miniaturized, modularized, and remotely actuated soft grippers. Adapted with permission.[17] Copyright 2021, The American Association for the Advancement of Science. (ii) Further developed kirigami grippers with ultra-delicacy, ultra-strength, and ultra-precision. Adapted under the terms of the Creative Commons CC-BY license.[127] Copyright 2023, The Authors. Published by Springer Nature.

While significant progress has been made in kirigami-based shape morphing structures, the inverse design remains a long-standing challenge due to the complexities associated with intricate cut patterns and the arrangement of non-periodic cut units at the local regions depending on the specific subject matter. In a shift from the conventional approach, Hong et al. have proposed a completely new concept, that is, to program curvatures through the cut boundaries as opposed to the design of intricate cut patterns.[19] By simply stretching a kirigami sheet with pre-defined curved cut boundaries, a spectrum of prescribed 3D curved shapes with various Gaussian curvatures can be achieved (as shown in Figure 6D). In contrast to previous kirigami designs with a network of polygon cut units, these kirigami sheets are composed of parallelly cut, discrete ribbons enclosed by continuous boundaries. This approach dexterously links the Gaussian curvature with the geodesic curvature along the boundary (i.e., the projection of boundary curvature), thereby facilitating a straightforward forward and inverse design methodology for desired 3D curvatures. When multiple sheets of semi-circular 2D precursors are layered together, followed by stretching, a floral pattern characterized by multilayered petals emerges. More interestingly is that the dynamic shape-morphing capabilities enabled by stretching allow for the grasping of an object (see Figure 6E), which was first demonstrated by Yang et al.[17] through simple cuts. Leveraging the precise control of the shape and the trajectory of kirigami through the cut boundary, Hong et al.[127]. have further developed this concept toward a universal, adaptable, multifunction, yet robust kirigami gripper. It can perform ultra-delicate, ultra-robust, and ultra-precise grasping tasks, including handling fragile liquids with minimal contact pressure (as low as 0.05 kPa), lifting objects up to 16,000 times their own weight, and adeptly grasping extremely thin and flexible items, such as 2-μm-diameter microfibers, on a flat substrate.

3.4. Bistability and Multistability

Bistable or multistable structures exhibit two or more equilibrium states with local minimum energy, allowing them to hold one of two or more states without the need for any external force to maintain the state. Switching between these states usually requires a significant force or a specific type of stimulation and

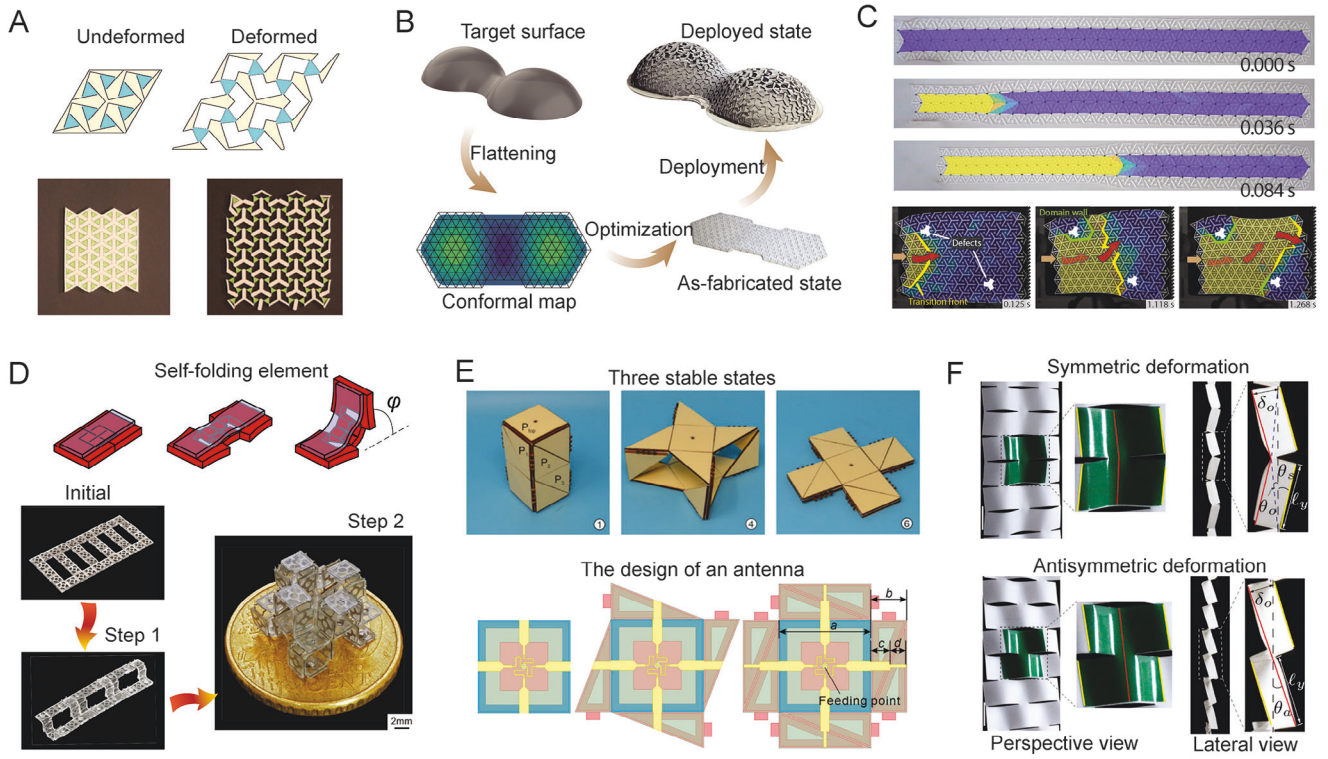

Figure 7. Kirigami-inspired bistable and multistable metamaterials. A) Ancient motifs inspired kirigami, which consists of an array of reentrant elements connected by a system of rotating units via compliant hinges, exhibits simultaneous auxeticity and structural bistability. Adapted with permission.[53] Copyright 2016, Elsevier. B) Bistable auxetic surface for stable shape transformation and deployment. The structure can be flat-fabricated using elastic sheet material and deployed toward a desired shape by triggering the bistable mechanism within the component units. Adapted with permission.[137] Copyright 2021, Association for Computing Machinery. C) Multistable structures capable of mimicking the material's property of phase propagation at the structural level. The structural analogs allow for precise manipulation of the direction, shape, and speed of the transition front by strategically adjusting the geometry and energy landscape of the fundamental building blocks. Adapted with permission.[77] Copyright 2020, National Academy of Science. D) Self-folding origami enabled by bilayer kirigami, which presents multiple stable configurations only requiring global stretching. Adapted with permission.[138] Copyright 2020, Elsevier. E) Tristable kirigami cuboid whose tristability arises from the strategically designed hinges. This design leads to the creation of a frequency-reconfigurable antenna with operation frequencies centered at 4.84, 3.48, and 2.58 GHz, respectively. Adapted with permission.[139] Copyright 2022, National Academy of Science. F) Multistable kirigami structures enabled by a selection of symmetric and asymmetric deformation. Adapted with permission.[75] Copyright 2018, American Physical Society.

is often accompanied by rapid snap-through instabilities. These unique characteristics have been leveraged in a vast number of applications including soft robotics,[132,133] energy harvesters,[134] energy absorbers,[135] and microelectromechanical systems.[136] Bistability and multistability in mechanical metamaterials typically arise from geometry-induced frustration in the forms of constrained beams, double-curved shells, and mechanism-based units, where certain geometric or mechanical constraints are inherently in conflict to prevent the switching between different stable states. Kirigami, emerging as a promising framework for designing metamaterials, has further enriched the possibility of constructing multistable materials.

Materials with auxetic properties exhibit the unconventional characteristic of thickening upon stretching due to their negative Poisson's ratio, making them ideal for designing shape-transforming metamaterials. Yet, many auxetic designs are monostable, reverting to their original configuration once the load is removed. Inspired by ancient geometric motifs, **Figure 7**A demonstrates a class of switchable architected materials exhibiting auxeticity and structural bistability simultaneously.[53] This design consists of a system of reentrant units connected by an array of rotating triangles or squares via compliant hinges. The reentrant units induced geometric frustration confers the structural bistability, whereas the cooperative rotation of the rotating units imparts the auxeticity. The tunable bistability and auxeticity are dictated by the geometry of the reentrant units, rotating units, and compliant hinges. Remarkably, this mechanism is also exploited to realize bistable shape-morphing structures, as illustrated in Figure 7B.[137] Empowered by an inverse design algorithm, a given target surface can be flattened into a plane encoded with optimized bistable auxetic cells. This structure is first manufactured in a flat form using an elastic material. Then, by using the bistable mechanism inherent to the individual cells, it can be deployed to achieve the desired double-curved shapes. Importantly, the bistability allows for the structure to be deployed without requiring intricate external supports or restrictive boundary conditions.

This bistable building block can be further employed to mimic material-level phenomena using macroscopically architected materials. Transition fronts propagating through solids and fluids

are ubiquitous in natural materials systems with nonconvex energy landscapes. Kirigami-based metamaterials with tailorable energy landscapes are capable of mimicking this phenomenon in various dimensions at the structural level.[77] In contrast to materials, the structural analogs allow for precise manipulation of the direction, shape, and speed of the transition front by strategically adjusting the geometry and energy landscape of the fundamental building blocks, as well as employing the interaction of transition fronts with lattice defects. As shown in Figure 7C, the multistable 1D network can automatically transform from a strained equilibrium state of higher strain energy to the unstrained ground state under certain perturbations, and the transition front in 2D structure can be further controlled via spatially introduced lattice defects. The same principles can be applied to 3D unit cells, which widens the untapped design space for reconfigurable structures and guided motions in various environments.

The self-folding of complex structures from flat states provides the potential to infuse various surface-related functionalities into the resulting 3D devices. However, most existing methodologies are constrained to simple folding sequences, specific materials, or large lengthscales, making them unsuitable for designing microscale metamaterials and devices with complex geometries. Figure 7D presents a mechanical self-folding technique that only requires global stretching for activation to create self-folding origami structures.[138] This structure is composed of a multistable kirigami element bonded to an elastic layer, both of which extend upon stretching. However, they respond differently when the stretch is removed. The elastic layer naturally tends to revert to its original length, but the bistable kirigami element cannot deform back by itself. This inability stems from an energy barrier caused by geometric frustration, resulting in the kirigami element being folded out-of-plane by the elastic layer. Thereby, the folding angle of each element can be readily programmed by tuning the geometry of the kirigami pattern and the dimension of the elastic layer. Tesselation of these elements in a modular manner enables the creation of multiple complex 3D structures at various length scales.

A vast majority of structures attain multistability through the integration of multiple bistable units in parallel or series configurations; few exhibit multistability at the single-unit level. Folding and cutting add a new dimension to creating multistable designs. As demonstrated in Figure 7E, a kirigami cuboid presents tristability from the strategically designed hinges.[139] Unlike conventional multistable structures comprising an array of bistable units, the kirigami cuboid exhibits generic tristability by itself. The kirigami cuboid consists of 18 rigid facets connected via three types of hinges, all of which remain unstretched in the three stable states. However, during the transition between the three stable states, at least one type of the hinges is under tension, leading to a triple-well energy landscape with zero energy at the minimum. Tessellating the units in series results in a new family of metamaterials with an exponentially increased number of stable states. This tristable unit has been further developed to create frequency-reconfigurable antennas suitable for 5G communication. The design is capable of achieving operation frequencies centered at 4.84, 3.48, and 2.58 GHz, respectively.

Another form of kirigami structures only shows multistability under certain conditions. As depicted in Figure 7F, the kirigami sheet with linear parallel cuts exhibits different buckling modes under stretching, i.e., symmetric, asymmetric deformation, and the coexistence of both.[75] These modes are determined by the geometry of the cuts and can be reversibly switched by external perturbations such as mechanical indentation. By locally and reversibly switching the deformation mode of unit cells, the material stiffness can be precisely programmed. Further, the use of bistable kirigami design in combination with reflective coating and thermally responsive materials paves the way for designing energy-neutral, environmentally responsive building envelopes,[140] where kirigami sheets can spontaneously switch the tilting direction in response to changes in environmental temperatures.

4. Prospective

The kirigami approach has substantially enriched the design space of 2D sheets, enabling a broad range of properties that were previously inaccessible. By integrating the kirigami principles with cutting-edge manufacturing techniques and advancements in materials science, one can achieve solutions that are flexible, adaptable, and transformative. This not only broadens our understanding of material manipulation but also paves the way for the development of innovative products for real-world applications. As research in this area progresses, kirigami-inspired metamaterials will reshape the landscape of several scientific domains.

First, kirigami-inspired metamaterials could potentially serve as platforms for mechanical computing and information processing. Mechanical computing and information processing is an emergent field that uses mechanical mechanisms and associated non-linearities instead of digital electronic hardware to compute and process information.[141–143] Recent research has revealed that crumpled sheets and amorphous media can encode memory effects and emergent computing capabilities but are difficult to control due to the highly disordered geometry of these systems.[144,145] Kirigami, with its rich nonlinear mechanical behaviors, well-prescribed deformation mechanisms, and readily programmable geometries, emerges as a promising alternative. Due to the tessellated nature and the programmable non-linearity of kirigami, each periodic unit could be engineered as a mechanical bit. The intricate interaction between these units makes kirigami a promising framework to store and process certain information and realize mechanical counting and computing (**Figure 8**A). This principle could pave the way for the design of purely mechanical automata without any electronics, facilitating the development of robots that operate in hazardous environments where sparks could trigger explosions, or for medical robots that navigate within the human body without the need for any batteries.

Another promising direction lies in the design of intelligent materials that are capable of adjusting their mechanical properties in response to various stimuli, inferring, and adapting to environments. For instance, the deformation of the kirigami is primarily dictated by the cut pattern. Once an array of cuts are introduced to the sheets, their mechanical property cannot be changed significantly. However, by integrating the kirigami principles with self-healing materials, certain cuts can be selectively healed and re-sutured under specific stimuli. This would significantly alter the response of the kirigami sheets, allowing them

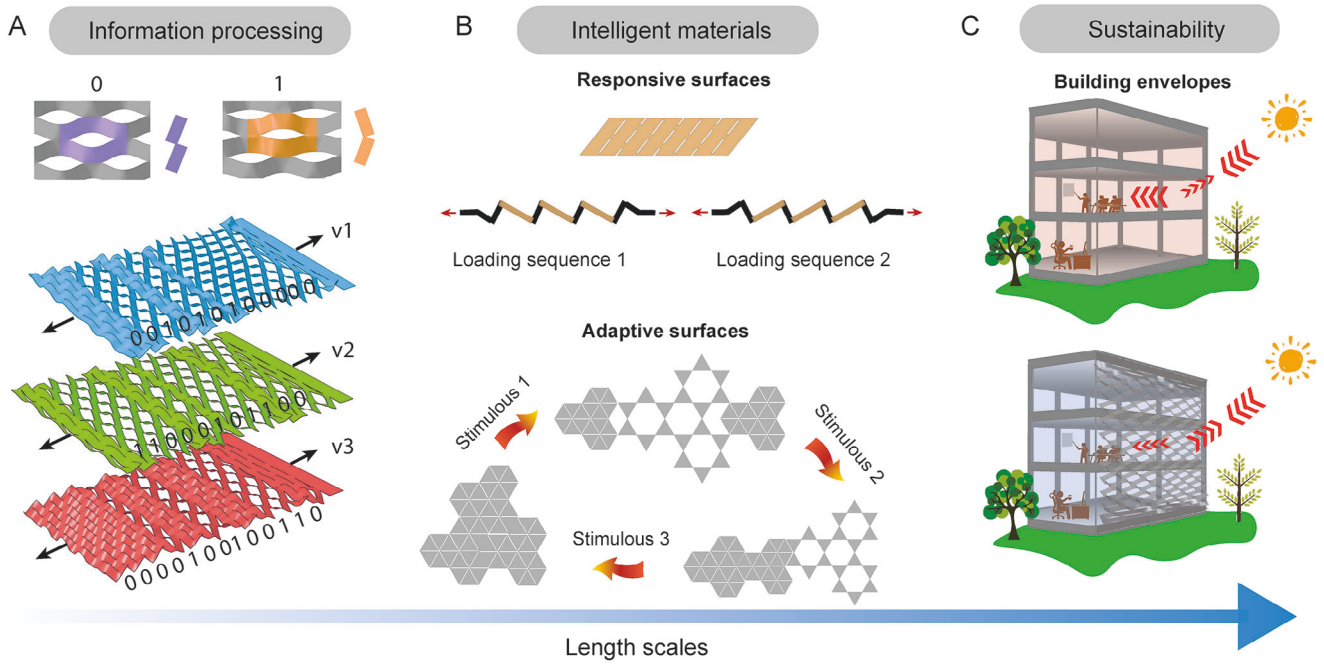

Figure 8. Potential applications and future advancements of kirigami. A) The tessellated nature and the programmable non-linearity of kirigami promise the potential for mechanical computing and information processing. B) Kirigami-inspired metamaterials exhibit tailored intelligence, allowing them to adapt their physical properties in response to environmental changes. C) Owing to its versatility and adaptability, kirigami could be a promising platform for designing sustainable devices.

to adapt to complex environments for more sustainable functions (Figure 8B). Jolly et al.[146] have demonstrated that a generalized kagome lattice, fabricated from shape memory polymers, can effectively decouple the topological response of a dynamic metamaterial from its kinematic stress history. This decoupling is pivotal for potential applications in devices such as switchable acoustic diodes and tunable vibration isolators. Yet, these initial explorations represent merely a fraction of the conceivable design space.

Furthermore, kirigami has the potential to foster the development of energy-efficient and eco-friendly devices. For instance, the exceptional stretchability, adaptability, and conformability of kirigami could be leveraged to design smart building envelops capable of self-cooling[140,147,148] (Figure 8C), large-scale structures that facilitate water collection in open environments,[37,149] and light-responsive solar panels that can automatically track sunlight to maximum the efficiency.[150] Additionally, by integrating physical intelligence into kirigami-based metamaterials and constructing them using biodegradable materials, one can reduce the electronic waste in certain devices, such as soft robotics and medical devices, steering us toward a more sustainable future. Nevertheless, bridging the gap between these innovative design principles and their practical implementation remains a significant, yet unresolved challenge.

While the strategically designed cuts grant kirigami structures high levels of flexibility, stretchability, adaptability, and conformability, they also compromise the mechanical properties of the structures. Maintaining the distinctive properties of kirigami without sacrificing strength and robustness remains a significant challenge. Efforts have been made to overcome these challenges by utilizing nacre-inspired strategies[38] and integrating self-locking mechanisms[151] to achieve a high mechanical strength-to-weight ratio or using geometrical optimization to enhance durability.[152,153]

Lastly, most of the demonstrations of kirigami structures are laboratory prototypes that are far from large-scale production and commercialization, where manufacturability, gravity, and cost will play important roles. So far, the constituent material's intrinsic properties have been overlooked in many kirigami designs. Addressing these challenges necessitates a convergence approach that brings together materials scientists, mechanical engineers, electrical engineers, computer scientists, and designers all together.

This paper has outlined the basic mechanisms of kirigami and reviewed a range of promising applications, but the field is evolving and has vast potential. Our objective is to provide a glimpse into the versatility and scope of kirigami-inspired metamaterials. We hope that the fundamental mechanisms and unique properties of kirigami, along with the representative applications we reviewed here, will inspire the discovery of novel metamaterials and encourage the community to address the challenges posed by real-world applications.

Acknowledgements

The authors acknowledged the financial support from Army Research Offices (ARO) through the MURI program (ARO # W911-NF-1810327), and the National Science Foundation (NSF) Future Eco Manufacturing Research Grant (FMRG, # CMMI 2037097).

Conflict of Interest

The authors declare no conflict of interest.

Keywords

bistability, kirigami, metamaterials, shape morphing, stretchability, surface topography

Received: August 22, 2023
Revised: November 5, 2023
Published online:

[1] A. A. Zadpoor, *Mater. Horiz.* **2016**, *3*, 371.
[2] K. Bertoldi, V. Vitelli, J. Christensen, M. Van Hecke, *Nat. Rev. Mater.* **2017**, *2*, 1.
[3] M. Kadic, G. W. Milton, M. van Hecke, M. Wegener, *Nat. Rev. Phys.* **2019**, *1*, 198.
[4] X. Xia, C. M. Spadaccini, J. R. Greer, *Nat. Rev. Mater.* **2022**, *7*, 683.
[5] L. Xu, T. C. Shyu, N. A. Kotov, *Acs Nano* **2017**, *11*, 7587.
[6] S. J. Callens, A. A. Zadpoor, *Mater. Today* **2018**, *21*, 241.
[7] X. Ning, X. Wang, Y. Zhang, X. Yu, D. Choi, N. Zheng, D. S. Kim, Y. Huang, Y. Zhang, J. A. Rogers, *Adv. Mater. Interfaces* **2018**, *5*, 1800284.
[8] J. J. Park, P. Won, S. H. Ko, *Int. J. Pr. Eng. Man.-GT* **2019**, *6*, 147.
[9] S. Chen, J. Chen, X. Zhang, Z.-Y. Li, J. Li, *Light: Sci. Appl.* **2020**, *9*, 75.
[10] Y. Sun, W. Ye, Y. Chen, W. Fan, J. Feng, P. Sareh, in *Structures*, vol. *33*, Elsevier, Amsterdam **2021**, pp. 3633–3643.
[11] Z. Zhai, L. Wu, H. Jiang, *Appl. Phys. Rev.* **2021**, *8*, 4.
[12] A. K. Brooks, S. Chakravarty, M. Ali, V. K. Yadavalli, *Adv. Mater.* **2022**, *34*, 2109550.
[13] Z. Zhang, Z. Tian, Y. Mei, Z. Di, *Mater. Sci. Eng. R Rep.* **2021**, *145*, 100621.
[14] J. Tao, H. Khosravi, V. Deshpande, S. Li, *Adv. Sci.* **2023**, *10*, 2204733.
[15] Y.-C. Cheng, H.-C. Lu, X. Lee, H. Zeng, A. Priimagi, *Adv. Mater.* **2020**, *32*, 1906233.
[16] A. Rafsanjani, Y. Zhang, B. Liu, S. M. Rubinstein, K. Bertoldi, *Sci. Rob.* **2018**, *3*, eaar7555.
[17] Y. Yang, K. Vella, D. P. Holmes, *Sci. Rob.* **2021**, *6*, eabd6426.
[18] L. Jin, A. E. Forte, K. Bertoldi, *Adv. Sci.* **2021**, *8*, 2101941.
[19] Y. Hong, Y. Chi, S. Wu, Y. Li, Y. Zhu, J. Yin, *Nat. Commun.* **2022**, *13*, 530.
[20] Q. He, R. Yin, Y. Hua, W. Jiao, C. Mo, H. Shu, J. R. Raney, *Sci. Adv.* **2023**, *9*, eade9247.
[21] B. Gao, A. Elbaz, Z. He, Z. Xie, H. Xu, S. Liu, E. Su, H. Liu, Z. Gu, *Adv. Mater. Technologies* **2018**, *3*, 1700308.
[22] R. Sun, B. Zhang, L. Yang, W. Zhang, I. Farrow, F. Scarpa, J. Rossiter, *Appl. Phys. Lett.* **2018**, *112*, 25.
[23] K. Yamagishi, T. Nakanishi, S. Mihara, M. Azuma, S. Takeoka, K. Kanosue, T. Nagami, T. Fujie, *NPG Asia Mater.* **2019**, *11*, 80.
[24] H. Wang, Z. Zhao, P. Liu, X. Guo, *Theor. App. Mech. Lett.* **2021**, *11*, 100240.
[25] W. Cho, J. Jeon, W. Eom, J. G. Lee, D.-G. Kim, Y. S. Kim, T. H. Han, J. J. Wie, *Adv. Funct. Mater.* **2021**, *31*, 2102106.
[26] K. Yong, S. De, E. Y. Hsieh, J. Leem, N. R. Aluru, S. Nam, *Mater. Today* **2020**, *34*, 58.
[27] K. Meng, X. Xiao, Z. Liu, S. Shen, T. Tat, Z. Wang, C. Lu, W. Ding, X. He, J. Yang, J. Chen, *Adv. Mater.* **2022**, *34*, 2202478.
[28] S. Jiang, X. Liu, J. Liu, D. Ye, Y. Duan, K. Li, Z. Yin, Y. Huang, *Adv. Mater.* **2022**, *34*, 2200070.
[29] T. Kim, Y.-G. Lee, *Sci. Rep.* **2018**, *8*, 13911.
[30] S. Babaee, Y. Shi, S. Abbasalizadeh, S. Tamang, K. Hess, J. E. Collins, K. Ishida, A. Lopes, M. Williams, M. Albaghdadi, A. M. Hayward, G. Traverso, *Nat. Mater.* **2021**, *20*, 1085.
[31] Z. Song, X. Wang, C. Lv, Y. An, M. Liang, T. Ma, D. He, Y.-J. Zheng, S.-Q. Huang, H. Yu, H. Jiang, *Sci. Rep.* **2015**, *5*, 10988.
[32] Y. Bao, G. Hong, Y. Chen, J. Chen, H. Chen, W.-L. Song, D. Fang, *ACS Appl. Mater. Interfaces* **2019**, *12*, 780.
[33] W.-J. Song, S. Yoo, G. Song, S. Lee, M. Kong, J. Rim, U. Jeong, S. Park, *Batter Supercaps* **2019**, *2*, 181.
[34] S. Qu, B. Liu, J. Wu, Z. Zhao, J. Liu, J. Ding, X. Han, Y. Deng, C. Zhong, W. Hu, *ACS Appl. Mater. Interfaces* **2020**, *12*, 54833.
[35] H. Liu, H. Li, Z. Wang, X. Wei, H. Zhu, M. Sun, Y. Lin, L. Xu, *Adv. Mater.* **2022**, *34*, 2207350.
[36] S. Jiang, J. Liu, W. Xiong, Z. Yang, L. Yin, K. Li, Y. Huang, *Adv. Mater.* **2022**, *34*, 2204091.
[37] J. Li, R. Ran, H. Wang, Y. Wang, Y. Chen, S. Niu, P. E. Arratia, S. Yang, *Nat. Commun.* **2021**, *12*, 5484.
[38] L. Jin, M. Yeager, Y.-J. Lee, D. J. O'Brien, S. Yang, *Sci. Adv.* **2022**, *8*, eabq3248.
[39] P. Z. Hanakata, E. D. Cubuk, D. K. Campbell, H. S. Park, *Phys. Rev. Res.* **2020**, *2*, 042006.
[40] G. Chaudhary, L. Niu, Q. Han, M. Lewicka, L. Mahadevan, *Proc. R. Soc. A* **2023**, *479*, 20220822.
[41] A. Rafsanjani, K. Bertoldi, *Phys. Rev. Lett.* **2017**, *118*, 084301.
[42] T. C. Shyu, P. F. Damasceno, P. M. Dodd, A. Lamoureux, L. Xu, M. Shlian, M. Shtein, S. C. Glotzer, N. A. Kotov, *Nat. Mater.* **2015**, *14*, 785.
[43] M. Isobe, K. Okumura, *Sci. Rep.* **2016**, *6*, 24758.
[44] Z. Yan, F. Zhang, F. Liu, M. Han, D. Ou, Y. Liu, Q. Lin, X. Guo, H. Fu, Z. Xie, M. Gao, Y. Huang, J. Kim, Y. Qiu, K. Nan, J. Kim, P. Gutruf, H. Luo, A. Zhao, K.-C. Hwang, Y. Huang, Y. Zhang, J. A. Rogers, *Sci. Adv.* **2016**, *2*, e1601014.
[45] H. Fu, K. Nan, W. Bai, W. Huang, K. Bai, L. Lu, C. Zhou, Y. Liu, F. Liu, J. Wang, M. Han, Z. Yan, H. Luan, Y. Zhang, Y. Zhang, J. Zhao, X. Cheng, M. Li, J. W. Lee, Y. Liu, D. Fang, X. Li, Y. Huang, Y. Zhang, J. A. Rogers, *Nat. Mater.* **2018**, *17*, 268.
[46] Y. Zhang, Z. Yan, K. Nan, D. Xiao, Y. Liu, H. Luan, H. Fu, X. Wang, Q. Yang, J. Wang, W. Ren, H. Si, F. Liu, L. Yang, H. Li, J. Wang, X. Guo, H. Luo, L. Wang, Y. Huang, J. A. Rogers, *Proc. Natl. Acad. Sci.* **2015**, *112*, 11757.
[47] Y. Zhang, F. Zhang, Z. Yan, Q. Ma, X. Li, Y. Huang, J. A. Rogers, *Nat. Rev. Mater.* **2017**, *2*, 1.
[48] S. Xu, Z. Yan, K.-I. Jang, W. Huang, H. Fu, J. Kim, Z. Wei, M. Flavin, J. McCracken, R. Wang, A. Badea, Y. Liu, D. Xiao, G. Zhou, J. Lee, H. U. Chung, H. Cheng, W. Ren, A. Banks, X. Li, U. Paik, R. G. Nuzzo, Y. Huang, Y. Zhang, J. A. Rogers, *Science* **2015**, *347*, 154.
[49] J. N. Grima, R. Jackson, A. Alderson, K. E. Evans, *Adv. Mater.* **2000**, *12*, 1912.
[50] J. N. Grima, A. Alderson, K. Evans, *Phys. Status Solidi B* **2005**, *242*, 561.
[51] G. W. Milton, *J. Mech. Phys. Solids* **2013**, *61*, 1543.
[52] Y. Tang, J. Yin, *Extreme Mech. Lett.* **2017**, *12*, 77.
[53] A. Rafsanjani, D. Pasini, *Extreme Mech. Lett.* **2016**, *9*, 291.
[54] L. Liu, G. P. Choi, L. Mahadevan, *Proc. R. Soc. A* **2021**, *477*, 20210161.
[55] Y. Cho, J.-H. Shin, A. Costa, T. A. Kim, V. Kunin, J. Li, S. Y. Lee, S. Yang, H. N. Han, I.-S. Choi, D. J. Srolovitz, *Proc. Natl. Acad. Sci.* **2014**, *111*, 17390.
[56] T. Castle, Y. Cho, X. Gong, E. Jung, D. M. Sussman, S. Yang, R. D. Kamien, *Phys. Rev. Lett.* **2014**, *113*, 245502.
[57] D. M. Sussman, Y. Cho, T. Castle, X. Gong, E. Jung, S. Yang, R. D. Kamien, *Proc. Natl. Acad. Sci.* **2015**, *112*, 7449.
[58] T. Castle, D. M. Sussman, M. Tanis, R. D. Kamien, *Sci. Adv.* **2016**, *2*, e1601258.
[59] X. Wang, S. D. Guest, R. D. Kamien, *Phys. Rev. X* **2020**, *10*, 011013.
[60] E. D. Demaine, J. O'Rourke, *Combinatorial Comput. Geom.* **2005**, *52*, 167.
[61] P. M. Dodd, P. F. Damasceno, S. C. Glotzer, *Proc. Natl. Acad. Sci.* **2018**, *115*, E6690.
[62] Y.-K. Lee, Z. Xi, Y.-J. Lee, Y.-H. Kim, Y. Hao, H. Choi, M.-G. Lee, Y.-C. Joo, C. Kim, J.-M. Lien, I.-S. Choi, *Sci. Adv.* **2020**, *6*, eaax6212.

[63] R. Straub, H. Prautzsch, Karlsruhe Reports in Informatics **2011**, *36*.
[64] S. Takahashi, H.-Y. Wu, S. H. Saw, C.-C. Lin, H.-C. Yen, in *Computer Graphics Forum*, vol. *30*, Wiley Online Library, Hoboken, NJ, USA **2011**, pp. 2077–2086.
[65] Z. Xi, Y.-H. Kim, Y. J. Kim, J.-M. Lien, *Computers Graph.* **2016**, *58*, 139.
[66] X. Guo, H. Li, B. Yeop Ahn, E. B. Duoss, K. J. Hsia, J. A. Lewis, R. G. Nuzzo, *Proc. Natl. Acad. Sci.* **2009**, *106*, 20149.
[67] S. Pandey, M. Ewing, A. Kunas, N. Nguyen, D. H. Gracias, G. Menon, *Proc. Natl. Acad. Sci.* **2011**, *108*, 19885.
[68] A. Azam, K. E. Laflin, M. Jamal, R. Fernandes, D. H. Gracias, *Biomed. Microdevices* **2011**, *13*, 51.
[69] L. Ionov, *Soft Matter* **2011**, *7*, 6786.
[70] Y.-K. Lee, Y. Hao, Z. Xi, W. Kim, Y. Park, K.-J. Cho, J.-M. Lien, I.-S. Choi, *PNAS Nexus* **2023**, *2*, pgad022.
[71] R. Fernandes, D. H. Gracias, *Adv. Drug Delivery Rev.* **2012**, *64*, 1579.
[72] S. Felton, M. Tolley, E. Demaine, D. Rus, R. Wood, *Science* **2014**, *345*, 644.
[73] N. An, A. G. Domel, J. Zhou, A. Rafsanjani, K. Bertoldi, *Adv. Funct. Mater.* **2020**, *30*, 1906711.
[74] Z. Yan, F. Zhang, J. Wang, F. Liu, X. Guo, K. Nan, Q. Lin, M. Gao, D. Xiao, Y. Shi, Y. Qiu, H. Luan, J. H. Kim, Y. Wang, H. Luo, M. Han, Y. Huang, Y. Zhang, J. A. Rogers, *Adv. Funct. Mater.* **2016**, *26*, 2629.
[75] Y. Yang, M. A. Dias, D. P. Holmes, *Phys. Rev. Mater.* **2018**, *2*, 110601.
[76] S. Babaee, S. Pajovic, A. Rafsanjani, Y. Shi, K. Bertoldi, G. Traverso, *Nat. Biomed. Eng.* **2020**, *4*, 778.
[77] L. Jin, R. Khajehtourian, J. Mueller, A. Rafsanjani, V. Tournat, K. Bertoldi, D. M. Kochmann, *Proc. Natl. Acad. Sci.* **2020**, *117*, 2319.
[78] N. Yang, M. Zhang, R. Zhu, *Extreme Mech. Lett.* **2020**, *40*, 100912.
[79] N. Wei, Y. Chen, K. Cai, J. Zhao, H.-Q. Wang, J.-C. Zheng, *Carbon* **2016**, *104*, 203.
[80] H. Heo, S. Li, H. Bao, J. Ju, *Adv. Eng. Mater.* **2019**, *21*, 1900225.
[81] H. Ouyang, Y. Gu, Z. Gao, L. Hu, Z. Zhang, J. Ren, B. Li, J. Sun, Y. Chen, X. Ding, *Phys. Rev. Appl.* **2023**, *19*, L011001.
[82] Y. Li, X. Song, H. Liu, J. Yin, *Extreme Mech. Lett.* **2021**, *49*, 101483.
[83] P. Cao, W. Ou, Y. Su, Y. Yin, E. Dong, Z. Song, J. Li, Y. Zhang, *Phys. Rev. Appl.* **2022**, *18*, 054040.
[84] H. Khosravi, S. Li, *Phys. Rev. Appl.* **2022**, *17*, 064054.
[85] Z. Liu, H. Du, J. Li, L. Lu, Z.-Y. Li, N. X. Fang, *Sci. Adv.* **2018**, *4*, eaat4436.
[86] W. J. Choi, G. Cheng, Z. Huang, S. Zhang, T. B. Norris, N. A. Kotov, *Nat. Mater.* **2019**, *18*, 820.
[87] S. Chen, Z. Liu, H. Du, C. Tang, C.-Y. Ji, B. Quan, R. Pan, L. Yang, X. Li, C. Gu, X. Zhang, Y. Yao, J. Li, N. X. Fang, J. Li, *Nat. Commun.* **2021**, *12*, 1299.
[88] L. Liu, S. Niu, J. Zhang, Z. Mu, J. Li, B. Li, X. Meng, C. Zhang, Y. Wang, T. Hou, Z. Han, S. Yang, L. Ren, *Adv. Mater.* **2022**, *34*, 2200823.
[89] R. Zhao, S. Lin, H. Yuk, X. Zhao, *Soft Matter* **2018**, *14*, 2515.
[90] D. Hwang, C. Lee, X. Yang, J. M. Pérez-González, J. Finnegan, B. Lee, E. J. Markvicka, R. Long, M. D. Bartlett, *Nat. Mater.* **2023**, *22*, 1030.
[91] B. Jang, S. Won, J. Kim, J. Kim, M. Oh, H.-J. Lee, J.-H. Kim, *Adv. Funct. Mater.* **2022**, *32*, 2113299.
[92] Z. Rao, Y. Lu, Z. Li, K. Sim, Z. Ma, J. Xiao, C. Yu, *Nat. Electron.* **2021**, *4*, 513.
[93] Y. Hong, B. Wang, W. Lin, L. Jin, S. Liu, X. Luo, J. Pan, W. Wang, Z. Yang, *Sci. Adv.* **2021**, *7*, eabf0795.
[94] J. Liu, S. Jiang, W. Xiong, C. Zhu, K. Li, Y. Huang, *Adv. Funct. Mater.* **2022**, *32*, 2109214.
[95] D.-G. Hwang, K. Trent, M. D. Bartlett, *ACS Appl. Mater. Interfaces* **2018**, *10*, 6747.
[96] J. Archard, *Tribology* **1974**, *7*, 213.
[97] H. Assender, V. Bliznyuk, K. Porfyrakis, *Science* **2002**, *297*, 973.
[98] B. Xin, J. Hao, *Chem. Soc. Rev.* **2010**, *39*, 769.
[99] L. Gamble, A. Lamoureux, M. Shtein, *Appl. Phys. Lett.* **2020**, *117*, 25.
[100] X. Yan, Y. Jin, X. Chen, C. Zhang, C. Hao, Z. Wang, *Sci. China Phys., Mech. Astronomy* **2020**, *63*, 224601.
[101] L. F. Cooper, *J. Orosthetic Dentistry* **2000**, *84*, 522.
[102] X. Lai, J. Peng, Q. Cheng, A. P. Tomsia, G. Zhao, L. Liu, G. Zou, Y. Song, L. Jiang, M. Li, *Angew. Chem.* **2021**, *133*, 14428.
[103] J. Ju, H. Bai, Y. Zheng, T. Zhao, R. Fang, L. Jiang, *Nat. Commun.* **2012**, *3*, 1247.
[104] K.-C. Park, S. S. Chhatre, S. Srinivasan, R. E. Cohen, G. H. McKinley, *Langmuir* **2013**, *29*, 13269.
[105] M. Damak, K. K. Varanasi, *Sci. Adv.* **2018**, *4*, eaao5323.
[106] A. Rafsanjani, L. Jin, B. Deng, K. Bertoldi, *Proc. Natl. Acad. Sci.* **2019**, *116*, 8200.
[107] A. Lamoureux, K. Lee, M. Shlian, S. R. Forrest, M. Shtein, *Nat. Commun.* **2015**, *6*, 8092.
[108] A. E. Forte, D. Melancon, M. Zanati, M. De Giorgi, K. Bertoldi, *Adv. Funct. Mater.* **2023**, *33*, 2214897.
[109] R. F. Shepherd, F. Ilievski, W. Choi, S. A. Morin, A. A. Stokes, A. D. Mazzeo, X. Chen, M. Wang, G. M. Whitesides, *Proc. Natl. Acad. Sci.* **2011**, *108*, 20400.
[110] E. E. Evke, C. Huang, Y.-W. Wu, M. Arwashan, B. Lee, S. R. Forrest, M. Shtein, *Adv. Eng. Mater.* **2021**, *23*, 2001079.
[111] C. Wu, X. Wang, L. Lin, H. Guo, Z. L. Wang, *ACS Nano* **2016**, *10*, 4652.
[112] H. Khosravi, S. Li, *Adv. Mater. Technol.* **2023**, *8*, 2202129.
[113] Y. Wang, H. Cui, T. Esworthy, D. Mei, Y. Wang, L. G. Zhang, *Adv. Mater.* **2022**, *34*, 2109198.
[114] H. Kim, S.-k. Ahn, D. M. Mackie, J. Kwon, S. H. Kim, C. Choi, Y. H. Moon, H. B. Lee, S. H. Ko, *Mater. Today* **2020**, *41*, 243.
[115] Y. Liu, H. Du, L. Liu, J. Leng, *Smart Mater. Struct.* **2014**, *23*, 023001.
[116] F. Fiorito, M. Sauchelli, D. Arroyo, M. Pesenti, M. Imperadori, G. Masera, G. Ranzi, *Renewable Sustainable Energy Rev.* **2016**, *55*, 863.
[117] J. Pikul, S. Li, H. Bai, R. Hanlon, I. Cohen, R. F. Shepherd, *Science* **2017**, *358*, 210.
[118] E. Siéfert, E. Reyssat, J. Bico, B. Roman, *Nat. Mater.* **2019**, *18*, 24.
[119] H. Aharoni, Y. Xia, X. Zhang, R. D. Kamien, S. Yang, *Proc. Natl. Acad. Sci.* **2018**, *115*, 7206.
[120] Y. Wang, R. Yin, L. Jin, M. Liu, Y. Gao, J. Raney, S. Yang, *Adv. Funct. Mater.* **2023**, *33*, 2210614.
[121] E. Hajiesmaili, D. R. Clarke, *Nat. Commun.* **2019**, *10*, 183.
[122] Y. Kim, H. Yuk, R. Zhao, S. A. Chester, X. Zhao, *Nature* **2018**, *558*, 274.
[123] Y.-J. Lee, S. K. Kanchwala, H. Cho, J. C. Jolly, E. Jablonka, M. Tanis, R. D. Kamien, S. Yang, *Adv. Mater.* **2023**, *35*, 2208088.
[124] G. P. Choi, L. H. Dudte, L. Mahadevan, *Nat. Mater.* **2019**, *18*, 999.
[125] P. Celli, C. McMahan, B. Ramirez, A. Bauhofer, C. Naify, D. Hofmann, B. Audoly, C. Daraio, *Soft Matter* **2018**, *14*, 9744.
[126] L. Jin, A. E. Forte, B. Deng, A. Rafsanjani, K. Bertoldi, *Adv. Mater.* **2020**, *32*, 2001863.
[127] Y. Hong, Y. Zhao, J. Berman, Y. Chi, Y. Li, H. Huang, J. Yin, *Nat. Commun.* **2023**, *14*, 4625.
[128] N. R. Sinatra, C. B. Teeple, D. M. Vogt, K. K. Parker, D. F. Gruber, R. J. Wood, *Sci. Rob.* **2019**, *4*, eaax5425.
[129] B. Gorissen, D. Reynaerts, S. Konishi, K. Yoshida, J.-W. Kim, M. De Volder, *Adv. Mater.* **2017**, *29*, 1604977.
[130] M. Cianchetti, C. Laschi, A. Menciassi, P. Dario, *Nat. Rev. Mater.* **2018**, *3*, 143.
[131] S.-U. Kim, Y.-J. Lee, J. Liu, D. S. Kim, H. Wang, S. Yang, *Nat. Mater.* **2022**, *21*, 41.
[132] T. Chen, O. R. Bilal, K. Shea, C. Daraio, *Proc. Natl. Acad. Sci.* **2018**, *115*, 5698.
[133] L. Jin, Y. Yang, B. O. T. Maldonado, S. D. Lee, N. Figueroa, R. J. Full, S. Yang, *Adv. Intell. Sys.* **2023**, *5*, 2300039.

[134] R. L. Harne, K. Wang, *Smart Mater. Struct.* **2013**, *22*, 023001.
[135] S. Shan, S. H. Kang, J. R. Raney, P. Wang, L. Fang, F. Candido, J. A. Lewis, K. Bertoldi, *Adv. Mater.* **2015**, *27*, 4296.
[136] Y. Cao, M. Derakhshani, Y. Fang, G. Huang, C. Cao, *Adv. Funct. Mater.* **2021**, *31*, 2106231.
[137] T. Chen, J. Panetta, M. Schnaubelt, M. Pauly, *ACM Trans. Graph.* **2021**, *40*, 1.
[138] T. van Manen, S. Janbaz, M. Ganjian, A. A. Zadpoor, *Mater. Today* **2020**, *32*, 59.
[139] X. Zhang, J. Ma, M. Li, Z. You, X. Wang, Y. Luo, K. Ma, Y. Chen, *Proc. Natl. Acad. Sci.* **2022**, *119*, e2117649119.
[140] Y. Tang, G. Lin, S. Yang, Y. K. Yi, R. D. Kamien, J. Yin, *Adv. Mater.* **2017**, *29*, 1604262.
[141] H. Yasuda, P. R. Buskohl, A. Gillman, T. D. Murphey, S. Stepney, R. A. Vaia, J. R. Raney, *Nature* **2021**, *598*, 39.
[142] Z. Meng, H. Yan, M. Liu, W. Qin, G. M. Genin, C. Q. Chen, *Adv. Sci.* **2023**, *10*, 2301581.
[143] T. Mei, C. Q. Chen, *Nat. Commun.* **2023**, *14*, 5204.
[144] N. C. Keim, J. D. Paulsen, Z. Zeravcic, S. Sastry, S. R. Nagel, *Rev. Mod. Phys.* **2019**, *91*, 035002.
[145] D. Shohat, D. Hexner, Y. Lahini, *Proc. Natl. Acad. Sci.* **2022**, *119*, e2200028119.
[146] J. C. Jolly, B. Jin, L. Jin, Y. Lee, T. Xie, S. Gonella, K. Sun, X. Mao, S. Yang, *Adv. Sci.* **2023**, *10*, 2302475.
[147] H. Jung, M. Hou, B. Kang, Z. Wang, H. Choi, H. W. Lee, Y. Lee, D.-K. Lee, P. Lee, D. Aviv, H. Kim, S. Yang, Adv. Sustainable Syst., 2300253.
[148] S. Wang, Y. Dong, Y. Li, K. Ryu, Z. Dong, J. Chen, Z. Dai, Y. Ke, J. Yin, Y. Long, *Mater. Horiz.* **2023**, *10*, 4243.
[149] P.-B. Bintein, A. Cornu, F. Weyer, N. De Coster, N. Vandewalle, D. Terwagne, *npj Clean Water* **2023**, *6*, 54.
[150] A. Awasthi, A. K. Shukla, M. M. SR, C. Dondariya, K. Shukla, D. Porwal, G. Richhariya, *Energy Reports* **2020**, *6*, 392.
[151] H. Zhang, J. Paik, *Adv. Funct. Mater.* **2022**, *32*, 2107401.
[152] Y. Tang, G. Lin, L. Han, S. Qiu, S. Yang, J. Yin, *Adv. Mater.* **2015**, *27*, 7181.
[153] X. Shang, L. Liu, A. Rafsanjani, D. Pasini, *J. Mater. Res.* **2018**, *33*, 300.

Lishuai Jin currently is a postdoctoral researcher at AMOLF, The Netherlands, working with Prof. Martin van Hecke. He obtained his B.E. in Applied Mechanics (2014) and Ph.D. in Solid Mechanics (2020) from Tianjin University. During his doctoral studies, he conducted research under the supervision of Prof. Katia Bertoldi at Harvard University (2017-2020). Subsequently, he joined the University of Pennsylvania as a postdoctoral researcher in Prof. Shu Yang's lab from 2020 to 2022. His research focuses on instabilities in soft materials and architected structures, as well as the development of metamaterials and soft robots with novel functionalities.

Shu Yang is a Joseph Bordogna Professor of Engineering and Applied Science in the Department of Materials Science and Engineering at University of Pennsylvania. She received her B. S. degree in Materials Chemistry from Fudan University, China, and Ph. D. degree in Chemistry and Chemical Biology at Cornell University. She then joined Bell Laboratories, Lucent Technologies as a Member of Technical Staff before moving to University of Pennsylvania. Her research interests include synthesis and engineering of well-defined polymers and composite materials with controlled size, shape, and morphology over multiple length scales, study of their directed assembly and unique surface, optical, and mechanical properties, as well as their stimuli responsiveness.